# Normal forms, bifurcations and finiteness properties of vector fields

Christiane ROUSSEAU†

**CRM-2917**

October 2002

†Département de mathématiques et de statistique and CRM, Université de Montréal, C.P. 6128, Succursale Centre-ville, Montréal (Qué.), H3C 3J7, Canada

**Abstract**

This article will be published in the Proceedings of the Séminaire de mathématiques supérieures 2002 on the theme "Normal forms, bifurcations and finiteness properties of vector fields". It consists of the text of the lectures delivered by the author and makes the bridge between the three themes of the book. Analytic objects have local finiteness properties. Compactness of the phase space and parameter space allows to derive global finiteness properties. One of the important tools for studying local properties is normal forms, which are also a tool to study bifurcations. In many generic situations the changes of coordinates to normal forms diverge. We explain this phenomenon in the case of a generic parabolic fixed point of a diffeomorphism by constructing a complete modulus of analytic classification for a generic unfolding of the diffeomorphism: the limit dynamics is too complicated to be encoded in the simple normal form. So the point of view of bifurcations brings a new light on the divergence of the normalizing series. Finally we recall the program to prove the finiteness part of Hilbert's 16th problem for quadratic systems started in 1991 and we discuss its progress and what remains to be done.

**Résumé**

Cet article sera publié dans les Comptes-rendus du Séminaire de mathématiques supérieures 2002 sur le thème "Formes normales, bifurcations et propriétés de finitude des champs de vecteurs". Il consitue le texte des conférences données par l'auteure et fait le pont entre les 3 thèmes du livre. Les objets analytiques ont des propriétés locales de finitude. La compacité de l'espace des phases et de l'espace des paramètres permet de dériver des propriétés globales de finitude. Un outil important pour l'étude des propriétés locales est donné par les formes normales, lesquelles sont aussi un outil pour l'étude des bifurcations. Dans beaucoup de situations génériques les changements de coordonnées normalisants divergent. Nous expliquons ce phénomène dans le cas d'un point fixe parabolique générique d'un difféomorphisme en construisant un module complet de classification analytique pour un dépoiement générqiue du difféomorphisme : la dynamique limite est trop complexe pour être encodée dans la forme normale qui est trop simple. Le point de vue des bifurcations amène donc un nouvel éclairage sur la divergence des séries normalisantes. Enfin nous rappelons le programme pour montrer la partie finitude du 16e problème de Hilbert pour les systèmes quadratiques commencé en 1991, nous discutons les progrès accomplis et ce qui reste à faire.

# 1   Introduction and perspectives

The text of this lectures makes the bridge between the three themes of the book. Although not exclusively, the main context will be analytic vector fields and analytic families of vector fields. The following ideas will be leading our mathematical developments:

- **Analytic objects have local finiteness properties.** In our context we will be mainly interested to the finite cyclicity of graphics of planar vector fields.

- **Compactness of the space phase yields to global finiteness properties.**

- **Compactness of the parameter space yields uniform finiteness properties.**

The main tools to study a vector field locally are:

(1) The flow-box theorem in the neighborhood of a singular point;

(2) Blow-ups and normal forms near singular points. We can consider blow-ups and normal forms of a single vector field as well as blow-ups and normal forms of families of vector fields.

Let us consider for a moment the problem of the finite cyclicity of graphics of planar vector fields. The standard method is to "calculate a return map" and to show that it has a finite number of fixed points. This return map can be written as a composition of regular transitions and Dulac maps in the neighborhood of the singular points. In the very generic situations, rough normal forms are sufficient to conclude to finite cyclicity, while in the more degenerate cases more refined normal forms are needed. For instance to prove the finite cyclicity of a homoclinic point through a saddle with nonzero trace (i.e. of codimension 1) a $C^1$ normal form is sufficient to conclude that the homoclinic loop has cyclicity one. When however we consider homoclinic loops of higher codimension more refined normal forms are needed. $C^k$ normal forms are sufficient to treat the generic cases while analycity arguments are needed to treat the homoclinic loops with identity return map inside finite parameter analytic families of vector fields.

Let us consider a family $(v_\lambda)_{\lambda \in \Lambda}$ of vector fields with $v_{\lambda_0}(x_0) = 0$. A general principle which we want to push further is the following: **The most generic $v_{\lambda_0}$ is, the most we know about $v_\lambda$ in the neighborhood of $x_0$ for $\lambda$ near $\lambda_0$.** As an example we can consider a vector field $v_{\lambda_0}$ with two pure imaginary eigenvalues at $x_0$ and such that the first Lyapunov quantity is negative. Then we know that $v_\lambda$ has none (resp. exactly one) limit cycle in the neighborhood of $x_0$ for values of $\lambda$ for which the singular point $x_\lambda$ (such that $x_{\lambda_0} = x_0$) is attracting (resp. repelling). If however the first $k-1$ Lypaunov quantities vanish and the $k$-th Lyapunov quantity is nonzero many more phase portraits are allowed. Finally when $v_{\lambda_0}$ has a center at the origin the only thing we can say on $x_\lambda$ is that it is a monodromic singular point.

The subject of normal forms was started by Poincaré and normal forms have been studied extensively since. If the singular points are not too degenerate reasonably good results exist for:

- formal normal forms;

- $C^\infty$ normal forms for a single vector field;

- $C^k$ normal forms for families of vector fields.

**What about analytic normal forms?**

i) They are the tools for problems of analytic classification under analytic changes of coordinates.

ii) Understanding the analytic type of a vector field in the neighborhood of an elementary singular point is an essential ingredient of the proof by Ecalle and Ilyashenko of the Dulac conjecture, namely that a polynomial vector field has a finite number of limit cycles.

iii) In many situations formal normalizing changes of coordinates diverge.

**Some examples of orbital normal forms for which the formal normalizing change of coordinate can be divergent:**

(1) The resonant saddle:

$$\begin{aligned}
\dot{x} &= x(1 + au^k) \\
\dot{y} &= y(-\tfrac{p}{q} + (1-a)u^k)
\end{aligned} \qquad (1.1)$$

where $u = x^p y^q$ is the resonant monomial.

(2) The saddle-node of codimension $n$:

$$\begin{aligned}
\dot{x} &= x^{n+1} \\
\dot{y} &= \pm y(1 + ax^n).
\end{aligned} \qquad (1.2)$$

(3) The non resonant saddle:

$$\begin{aligned}
\dot{x} &= x \\
\dot{y} &= -\lambda y
\end{aligned} \qquad (1.3)$$

where $\lambda$ is a Liouvillian irrational positive number.

(4) The diffeomorphism $f : (C, 0) \to (C, 0)$ with a parabolic fixed point:

$$f(z) = z + z^{n+1} + o(z^n + 1). \qquad (1.4)$$

The common point to all these situations is that **divergence is the rule and convergence is the exception**. Such systems have been studied thoroughly for fixed values of the eigenvalues or of the multiplier: they form natural "families" of systems. In a series of papers by Ilyashenko ([19], [20]) we find theorems of the form: *Either the change of coordinates to normal form converges for all systems in the family or it diverges for the majority of systems (for almost all systems in the case of finite parameter families of systems).* Later, in the resonant cases, Ecalle [13] has given a more precise description of the subspace of parameter space where we can expect convergence.

As mentioned above in all these situations divergence is the rule and convergence is the exception. The question we want to consider is:

<div align="center">

**"WHY?"**

</div>

The answer proposed is in the following spirit: our normal form is a kind of "model".

- Divergence is the rule and convergence is the exception **because the "model" is to poor to encode the rich dynamics of the system.**

- So the rich dynamics is encoded in the divergent normalizing transformation. **How to read it?**

- If we can read this rich dynamics it will become obvious that the poor dynamics of the model is an exceptional case.

- If divergence is the generic situation then, by the principle described above, we should expect to be able to describe some properties of local perturbations of the system.

Let us go back in the past and look at the following citation of Abel [1] (Œuvres complètes de Niels Henrik Abel, tome 2, in the letters to Holmboe (1826), pages 256-257): *"Les séries divergentes sont en général quelque chose de bien fatal et c'est une honte qu'on ose y fonder aucune démonstration. On peut démontrer tout ce qu'on veut en les employant, et ce sont elles qui ont fait tant de malheurs et qui ont enfanté tant de paradoxes. . . . Enfin mes yeux se sont dessillés d'une manière frappante, car à l'exception des cas les plus simples, par exemple les séries géométriques, il ne se trouve dans les mathématiques presque aucune série infinie dont la somme soit déterminée d'une manière rigoureuse, c'est-à-dire que* **la partie la plus essentielle des mathématiques est sans fondement.** *Pour la plus grande partie les résultats sont justes il est vrai, mais c'est là une chose bien étrange. Je m'occupe à en chercher la raison, problème très intéressant.*

The author has been fascinated by this complete change in the dynamics of the subject: Nowadays divergent series occupy a marginal place inside mathematics and we remember Abel as a mathematician who banished the use of divergent series.

To study why generically so many series diverge the point of view which is taken here is to **unfold**: the bifurcation point of view will help us understand the normal forms. Indeed many situations where we encounter divergence are limit situations, for instance:

i) Irregular singular points of linear differential equations occur when regular points coallesce.

ii) A parabolic point of a diffeomorphism of $(C, 0)$ is a fixed point of multiplicity $n + 1 > 1$.

iii) A saddle-node is a multiple singular point.

iv) The holonomy of a separatrix of a non integrable resonant saddle with eigenvalues $1 : -1$ has a parabolic fixed point (hence a multiple fixed point) at the origin.

In these lectures we will address the following questions:

**Questions:**

(1) If the change of coordinates to normal form near $x_0$ diverges for $v_{\lambda_0}$ (i.e. we are in the generic situation):

- what can we say of $v_\lambda$ in the neighborhood of $x_0$ for $\lambda$ close to $\lambda_0$? (We look for the properties which depend only on the germ of $v_{\lambda_0}$ at $x_0$.)
- What analytic families $v_\lambda$ can unfold $v_{\lambda_0}$? More precisely can we give the moduli space of the space of such analytic families?

(2) Can we understand the dynamics of $v_{\lambda_0}$ from the fact that it is the limit of the $v_\lambda$ for $\lambda \to \lambda_0$?

Let us illustrate this on an example:

**The saddle-node:** By an analytic change of coordinates we can bring an analytic system with a saddle-node of multiplicity 2 to the normal form:

$$\begin{aligned} \dot{x} &= x^2 \\ \dot{y} &= y(1 + ax) + x^2 R(x, y). \end{aligned} \tag{1.5}$$

The formal normal form is our "model" (Figure 1a):

$$\begin{aligned} \dot{x} &= x^2 \\ \dot{y} &= y(1 + ax). \end{aligned} \tag{1.6}$$

One obstruction to bring (1.5) to (1.6) is the non-existence of an analytic center manifold. We now unfold: the "model family" for the unfolding is (Figure 1b)

$$\begin{aligned} \dot{x} &= x^2 - \epsilon \\ \dot{y} &= y(1 + a(\epsilon)x). \end{aligned} \tag{1.7}$$

To understand the dynamics we need to consider $x, y \in C$. Figure 2 represents the model and model family (only the $x$-variable is drawn as a 2-dimensional variable).
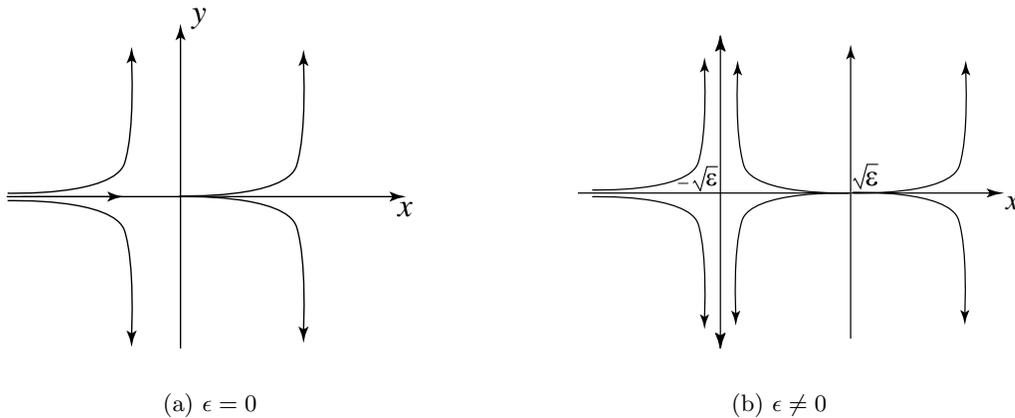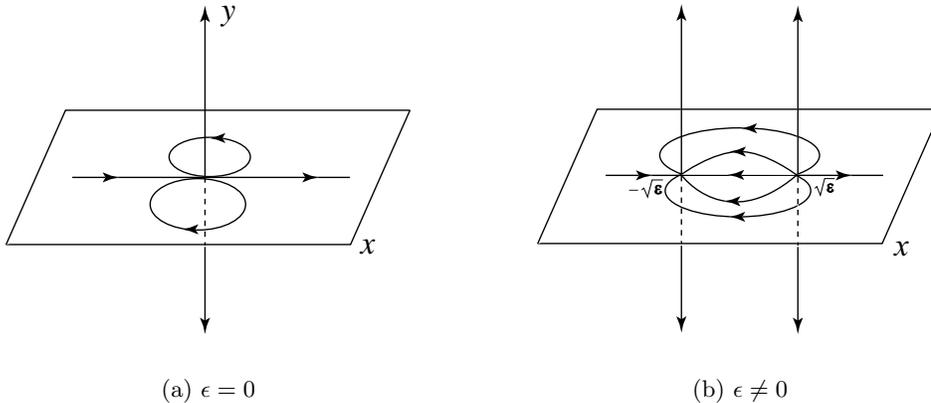


(a) $\epsilon = 0$          (b) $\epsilon \neq 0$

Figure 1: The "model"



(a) $\epsilon = 0$          (b) $\epsilon \neq 0$

Figure 2: The "model"

Let us now suppose that (1.5) has no analytic center manifold. The formal equation of the center manifold

$$y = \sum_{n=2}^{\infty} b_n x^n \tag{1.8}$$

is 1-summable in all directions except $R^+$ ([28]). This yields a "ramified" center manifold as in Figure 3a. To simplify we can suppose $a(\epsilon) \in R$, although this is not essential. Let now $\epsilon \in R^+$. The saddle point at $(-\sqrt{\epsilon}, 0)$ always has an invariant stable manifold which is necessarily ramified at the node as in Figure 3b.

Let us now look at the local model at the node: it is known since Poincaré that the change of coordinates to the local model is always convergent. We have two cases:
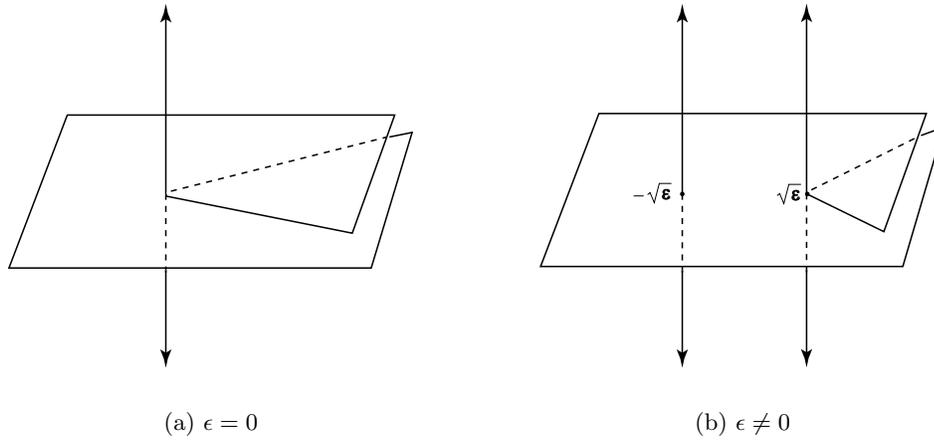
4

(a) $\epsilon = 0$          (b) $\epsilon \neq 0$

Figure 3: The invariant manifold

- **Non resonant node:** the normal form is linear

$$\begin{aligned} \dot{x} &= \lambda x \\ \dot{y} &= y, \end{aligned}$$

(1.9)

when $\lambda \notin 1/N$. Integral curves (except the $y$-axis) have equation

$$y = Cx^{1/\lambda}.$$

(1.10)

Hence all integral curves are ramified except $x = 0$ and $y = 0$ which are analytic. The divergence of the series (1.8) yields that the analytic separatrices of the saddle and of the node do not glue together. Here **divergence means incompatibility** (Figure 4).
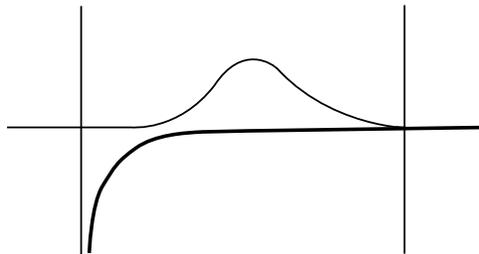


Figure 4: Incompatibility of the invariant analytic manifolds

- **Resonant node:** Here we have two cases. The exceptional case is when the node is linearizable

$$\begin{aligned} \dot{x} &= \tfrac{1}{n}x \\ \dot{y} &= y. \end{aligned}$$

(1.11)

In this case all integral curves (except $x = 0$) are of the form $y = Cx^n$. They are analytic, thus non ramified. Hence this case is necessarily excluded and we need be in the generic situation where the resonant monomial has a nonzero coefficient:

$$\begin{aligned} \dot{x} &= \tfrac{1}{n}x \\ \dot{y} &= y + bx^n, \end{aligned}$$

(1.12)

with $b \neq 0$. In this case the only non ramified integral curve is $x = 0$.

5

The conclusion is the following: **For some particular values of $\epsilon$ where one of the singular point is resonant the incompatibility implies some generic property of the unfolded point itself.** This observed phenomenon is very general: it is some form of *parametric resurgence*.

Similar resurgence phenomena occur at the saddle for parameter values for which it is resonant. We will learn to read them from the Martinet-Ramis modulus of analytic classification of the saddle-node.

We can of course extend to complex values of the parameter $\epsilon$. When the ratio of the eigenvalues at $(\pm\sqrt{\epsilon}, 0)$ is not real the singular points are linearizable and have exactly two analytic trajectories, all other integral curves being ramified. If the saddle-node has no analytic center manifold then we observe in the unfolding that **the two (weak) analytic separatrices of $(\pm\sqrt{\epsilon}, 0)$ do not coincide.** This was already observed by Glutsyuk [15]. **But we can not make a full turn in the parameter space as $\sqrt{\epsilon}$ and $-\sqrt{\epsilon}$ are exchanged. We cannot expect a description of the phenomenon analytic in $\epsilon$.**

The study of all these phenomena is done through the description of a complete modulus of analytic classification for generic analytic families unfolding a diffeomorphism with a generic parabolic point

$$f_\epsilon(z) = z + (z^2 - \epsilon)(1 + h(\epsilon, z)), \tag{1.13}$$

presented in detail in [27]. This allows to give an interpretation of all ingredients of the Ecalle-Voronin modulus of analytic classification of $f_0$.

## 1.1 The Ecalle-Voronin modulus of a generic diffeomorphism with a parabolic point

We describe the modulus of a germ of diffeomorphism

$$f_0(z) = z + z^2 + (1 - a)z^3 + o(z^3). \tag{1.14}$$

The modulus is composed of three parts:

- *The discrete part $k = 1$*: $k + 1$ is the multiplicity of the parabolic point. (Here we limit ourselves to the generic codimension 1 case.)

- *The formal part $a \in C$*: in the unfolding $a$ is unfolded as $a(\epsilon)$ depending analytically of $\epsilon$ and is interpreted as a *shift* between the two singular points. Indeed the two singular points may not be resonant simultaneously.

- *The analytic part*: we describe precisely the diffeomorphism by describing its orbit space. The diffeomorphism is topologically equivalent to the time-one map of the flow of the vector field $z^2 \frac{\partial}{\partial z}$ (see Figure 5).

  To describe the orbit space we give ourselves two "fundamental domains". To construct a *fundamental domain* we take a closed curve $l$ through the origin such that $l \cap f_0(l) = \{0\}$. The fundamental domain is the domain between $l$ and $f_0(l)$ where we identify $l$ and $f_0(l)$ through $z \equiv f_0(z)$. Then each orbit has at most one point in a fundamental domain. There is no way to represent all orbits by a unique fundamental domain and two fundamental domains are necessary to represent the whole space of orbits. But then some orbits have representatives in the two fundamental domains. To describe the orbit space we must identify points in the two fundamental domains which belong to the same orbit. This is done via a pair of maps defined respectively in the upper end and lower end of the fundamental domains (Figure 6).

  To describe these maps we use the fact that the fundamental domains are conformally equivalent to spheres $S^\pm$ with 0 and $\infty$ identified. Then there exist analytic diffeomorphisms $\psi^0, \psi^\infty : S^+ \to S^-$ defined in the neighborhood of 0 and $\infty$ such that the image of $w^+ \in S^+$ by $\psi^0$ or $\psi^\infty$ is a point of $S^-$ belonging to the same orbit as $w^+$. The diffeomorphisms $\psi^0$ and $\psi^\infty$ are defined up to choices of
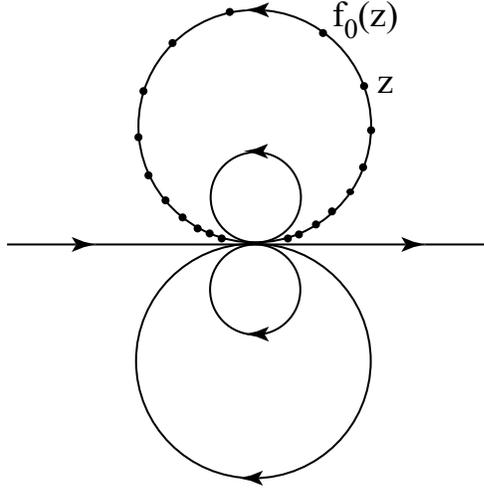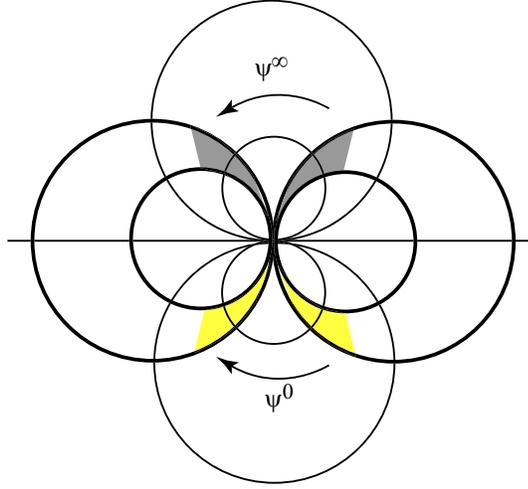
Figure 5: The diffeomorphism $f_0$



Figure 6: The two fundamental domains and identifying maps $\psi^0$ and $\psi^\infty$

coordinates on the spheres preserving $0$ and $\infty$, i.e. up to composition by linear maps in the source and target space. Then

$$(\psi_1^0, \psi_1^\infty) \equiv (\psi_2^0, \psi_2^\infty) \quad \text{iff} \quad \exists C, C' \in C^* \begin{cases} \psi_1^0(w) = C\psi_2^0(C'w) \\ \psi_1^\infty(w) = C\psi_2^\infty(C'w) \end{cases} \tag{1.15}$$

The analytic part of the modulus is given by the equivalence class $[\psi^0, \psi^\infty]$.

- The formal part $a$ (mod $2\pi i$) can be recovered from the analytic part since $(\psi^0)'(0)(\tilde{\psi}^\infty)'(0) = \exp(4\pi^2 a)$, where $\tilde{\psi}^\infty$ is $\psi^\infty$ viewed in the coordinate $1/w$. So the Ecalle-Voronin modulus is almost $(k = 1, [\psi^0, \psi^\infty])$.

To interpret the analytic part of the modulus we must describe the "normal form" of $f_0$, which we call the *model diffeomorphism.* It is given by the time-one map of the flow of the vector field

$$\frac{z^2}{1 + az} \frac{\partial}{\partial z}. \tag{1.16}$$

7

There always exist a change of coordinate conjugating $f_0$ to the model diffeomorphism. The formal change of coordinate can be summed to an analytic one if and only if $\psi^0$ and $\psi^\infty$ are linear. The reason why the time-one map of the flow of (1.16) is a model is because this diffeomorphism is "fully iterable": we can take its $n$-root for any $n$ and, more generally, define $f^{\circ c}$, where $c$ is a complex number.

**An interpretation of the analytic part of the modulus:** The nonlinearities of $\psi^0$ and $\psi^\infty$ control *parametric resurgence phenomena* in the unfolding (1.13). Then

- $\psi^0$ (resp. $\psi^\infty$) controls $-\sqrt{\epsilon}$ (resp. $\sqrt{\epsilon}$) when its multiplier is on the unit circle.

- If

$$\psi^\infty(w) = w + \sum_{n=2}^\infty b_n w_n \tag{1.17}$$

  then $\forall p, q, \in N$ with $1 \le q < p$ there exists polynomials

$$L_{p,q}^\infty(b_2, \ldots, b_{p+1}) \tag{1.18}$$

  such that if $L_{p,q}^\infty(b_2, \ldots, b_{p+1}), \ne 0$ then $f_\epsilon$ is non linearizable at $\sqrt{\epsilon}$ as soon as the multiplier $\lambda = f'_\epsilon(\sqrt{\epsilon})$ is of the form

$$\lambda = \exp(2\pi i \frac{p}{n}) \tag{1.19}$$

  with $n$ large and

$$n \equiv q \pmod{p}. \tag{1.20}$$

- If $\psi^\infty$ is nonlinear, then at least one of the $L_{p,q}^\infty(b_2, \ldots, b_{p+1}) \ne 0$.

- A similar result exists with $\psi^0$ controlling $-\sqrt{\epsilon}$. If $a \ne 0$ we cannot simultaneously scale $\psi^{\infty\prime}(0) = 1$ and $\psi^{0\prime}(0) = 1$.

## 1.2   An answer to a question of Martinet-Ramis

In [28] Martinet and Ramis study the modulus of a saddle-node. They show that the analytic type of a saddle-node is characterized by the analytic type of the holonomy of the strong separatrix, which is a diffeomorphism with a parabolic fixed point. However not all diffeomorphisms with a parabolic fixed point can be realized as the holonomy map of the strong separatrix of a saddle-node, yielding that the moduli space of the holonomy maps of strong separatrices of saddle-nodes is strictly smaller that the moduli space of diffeomorphims with a parabolic fixed point. Martinet and Ramis ask the following question: (the equation (2) to which they refer is our equation (1.5)): *"Un phénomène qui reste un peu surprenant à nos yeux est que les holonomies produites par les équations (2) ne sont pas arbitraires: on obtient seulement une "petite partie du module d'Ecalle". (Nous nous proposons de montrer dans un article ultérieur qu'il n'en est plus de même dans le cas des équations résonantes "non dégénérées" ($\lambda = -p/q \ne 0$): le module des classes d'équivalence analytiques d'équations différentielles s'identifie complètement au "module d'Ecalle")."*Indeed the modulus of the holonomy of the strong separatrix of a saddle-node has the form ($[\psi^0, \psi^\infty]$) where

$$\psi^\infty(w) = \frac{w}{1 - bw}. \tag{1.21}$$

The answer comes from the following theorem:

**1.1 Theorem** *[27] The only analytic function $\psi^\infty(w)$ of the form (1.17) for which*

$$\forall p > 1, \forall q \quad L_{p,q}^\infty(b_2, \ldots, b_{p+1}) = 0 \tag{1.22}$$

*is the Möbius function (1.21).*

**Hence the Möbius function is the only function which can reflect the very simple dynamics of the node in the unfolding.** Any other function would force the node to have a more complex dynamics, in particular to be nonlinearizable for non resonant cases.

## 2  Modulus of analytic classification of generic families unfolding a diffeomorphism with a generic parabolic point

We now present the results of [27]. We consider a generic diffeomorphism $f_0(z)$ with a parabolic fixed point as in (1.14). An unfolding is *generic* if

$$\left. \frac{\partial f_\epsilon}{\partial \epsilon} \right|_{\epsilon=0} \neq 0. \tag{2.1}$$

We classify germs of analytic families of diffeomorphims under *weak equivalence.*

### 2.1  Preliminaries

**2.1 Definition** Two germs $f_{1,\epsilon_1}(z)$ and $f_{2,\epsilon_2}(z)$ of analytic families of diffeomorphims are *weakly equivalent* if there exists a germ of bijective map $K = (h, H)$:

$$(\epsilon_1, z) \mapsto (h(\epsilon_1), H(\epsilon_1, z)) \tag{2.2}$$

fibered over the parameter space where:

i) $h$ is a germ of holomorphic diffeomorphism $(C, 0) \to (C, 0)$.

ii) there exists a representative $H(\epsilon_1, z)$ for $(z, \epsilon_1) \in U \times V$ such that

- $H_{\epsilon_1} = H(\epsilon_1, .)$ is analytic in $z$ for $z \in U$;
- $H_{\epsilon_1}$ conjugates $f_{1,\epsilon_1}$ and $f_{2,h(\epsilon_1)}$ over $U$, for all $\epsilon_1 \in V$, namely:

$$f_{2,h(\epsilon_1)}(H_{\epsilon_1}(z)) = H_{\epsilon_1}(f_{1,\epsilon_1}(z)). \tag{2.3}$$

We will show that if two generic families unfolding a diffeomorphism with a generic parabolic point are weakly equivalent, then they are equivalent in a stronger sense.

**"Preparation" of an unfolding $f_\epsilon(z)$ of $f_0(z)$.**
We can suppose that the two singular points are located at $\pm\sqrt{\epsilon}$, i.e. that $f_\epsilon(z)$ has the form (1.13). We want to compare our family with the "model family" which is given by the time-one map of the flow of the vector field

$$\frac{z^2 - \epsilon}{1 + a(\epsilon)z} \frac{\partial}{\partial z}. \tag{2.4}$$

(From now on we will not write the dependence of $a(\epsilon)$ and simply denote $a = a(\epsilon)$.) The singular points of (2.4) are $\pm\sqrt{\epsilon}$. Their eigenvalues are

$$\mu_\pm = \pm\frac{2\sqrt{\epsilon}}{1 \pm a\sqrt{\epsilon}} \tag{2.5}$$

9

and satisfy

$$
\begin{aligned}
\frac{1}{\sqrt{\epsilon}} &= \frac{1}{\mu_+} - \frac{1}{\mu_-} \\
a &= \frac{1}{\mu_+} + \frac{1}{\mu_-},
\end{aligned} \tag{2.6}
$$

i.e. in the model family $a$ and $\epsilon$ are analytic invariants.

We make a change of coordinate $(z, \epsilon) \mapsto (\bar{z}, \bar{\epsilon})$ in $f_\epsilon(z)$:

$$
\overline{f}_{\bar{\epsilon}}(\bar{z}) = \bar{z} + (\bar{z}^2 - \epsilon)\overline{h}(\bar{z}, \bar{\epsilon}), \tag{2.7}
$$

so that $\bar{\epsilon}$ becomes an analytic invariant, i.e.

$$
\frac{1}{\sqrt{\epsilon}} = \frac{1}{\ln \lambda_+} - \frac{1}{\ln \lambda_-}, \tag{2.8}
$$

where $\lambda_\pm$ are the multipliers at the singular points $\pm\sqrt{\epsilon}$ of (2.4), (in which we replace $(z, \epsilon)$ by $(\bar{z}, \bar{\epsilon})$). Then for the model family (2.4) we choose

$$
a(\epsilon) = \frac{1}{\ln \lambda_+} + \frac{1}{\ln \lambda_-}. \tag{2.9}
$$

The new family $\overline{f}_{\bar{\epsilon}}(\bar{z})$ is called "prepared". $\bar{\epsilon}$ is the canonical parameter of the family.

>From now on we will limit ourselves to prepared families (1.13). Because the parameter is an analytic invariant then **weak equivalence between prepared families must preserve the parameter.**

Here are some general principles to guide us in the definition of a complete modulus of analytic classification for prepared families:

- We must cover a whole neighborhood of the origin in parameter space.

- We try to have as much continuity and smoothness in $\epsilon$ as possible.

- But it may be difficult to make a full turn in $\epsilon$, so it is natural to work with the universal covering of the $\epsilon$-space.

## 2.2 Description of the modulus of analytic classification for the family

i) We give ourselves $\delta > 0$ arbitrarily small.

We consider the universal covering of the $\epsilon$-space with projection $\pi$ and call $\hat{\epsilon}$ the corresponding variable so that $\pi(\hat{\epsilon}) = \epsilon$.

ii) We describe the orbit space of a prepared family (1.13) for all neighborhoods $\{z; |z| < r\}$ with $r \leq r_0$, where $r_0$ depends on $\delta$, for all values of $\hat{\epsilon}$ such that

$$
\begin{cases}
|\hat{\epsilon}| < \rho < Kr \\
\arg \hat{\epsilon} \in (-\pi + \delta, 3\pi - \delta)
\end{cases} \tag{2.10}
$$

(Figure 7), where $K > 0$ is a positive constant depending on $r_0$ and $\delta$. This neighborhood covers only once the Siegel direction $R^-$. We call $V_\delta$ this sector.

A similar description can be done in a second sector

$$
\begin{cases}
|\hat{\epsilon}| < \rho < Kr \\
\arg \hat{\epsilon} \in (-3\pi + \delta, \pi - \delta).
\end{cases} \tag{2.11}
$$

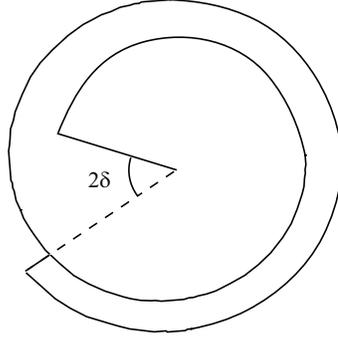The union of the two neighborhoods covers a full neighborhood of 0 in the $\sqrt{\epsilon}$-space.

10

Figure 7: The sector $V_\delta$ in $\hat{\epsilon}$-space

iii) $\forall \hat{\epsilon} \in V_\delta$ the orbit space is described by two crescents $C_\epsilon^\pm$, which:

- are fundamental domains for $f_\epsilon$;
- whose quotient by $f_\epsilon$ have the conformal structure of spheres $S_\epsilon^\pm$, the points $\sqrt{\epsilon}$ (resp. $-\sqrt{\epsilon}$) corresponding to $\infty$ (resp. $0$);
- in the two ends of the crescents, (i.e. near $0$ and $\infty$ on the spheres $S_\epsilon^\pm$) points are identified by germs of analytic diffeomorphisms $\psi_\epsilon^\infty$ and $\psi_\epsilon^0$ (Figure 8).
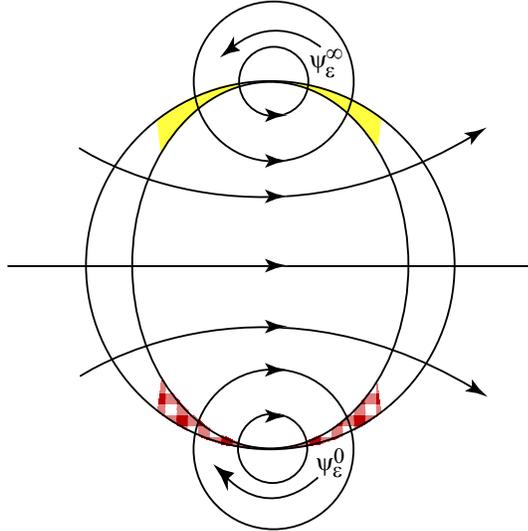


Figure 8: The two crescents and diffeomorphisms $\psi_\epsilon^\infty$ and $\psi_\epsilon^0$

iv) It is possible to choose the $C_\epsilon^\pm$ depending analytically on $\hat{\epsilon}$ for $\hat{\epsilon} \neq 0$ and continuously on $\hat{\epsilon}$ near $\hat{\epsilon} = 0$.

v) The cordinates on the spheres can be chosen so that the functions $\psi_\epsilon^\infty$ and $\psi_\epsilon^0$ depend analytically on $\hat{\epsilon}$ for $\hat{\epsilon} \neq 0$ and continuously on $\hat{\epsilon}$ near $\hat{\epsilon} = 0$.

vi) We define the usual equivalence relation

$$(\psi_{1,\epsilon}^0, \psi_{1,\epsilon}^\infty) \equiv (\psi_{2,\epsilon}^0, \psi_{2,\epsilon}^\infty) \quad \text{iff} \quad \exists C, C' \in C^* \begin{cases} \psi_{1,\epsilon}^0(w) = C\psi_{2,\epsilon}^0(C'w) \\ \psi_{1,\epsilon}^\infty(w) = C\psi_{2,\epsilon}^\infty(C'w) \end{cases} \tag{2.12}$$

11

vii) $\forall \hat{\epsilon} \in V_\delta$ $[(\psi_{\hat{\epsilon}}^0, \psi_{\hat{\epsilon}}^\infty)]$ is a complete modulus of analytic classification for $f_\epsilon$.

**2.2 Theorem** *[27] The family $\{[(\psi_{\hat{\epsilon}}^0, \psi_{\hat{\epsilon}}^\infty)]\}|_{\hat{\epsilon} \in V_\delta}$, together with $a(0)$, is a complete modulus of analytic classification of the family $\{f_\epsilon\}$.*

**Proof** We just give an idea of the proof: it is a generalization of ideas of Lavaurs and Shishikura (their method applies to smaller sectors in $\epsilon$-space as in Figure 9).
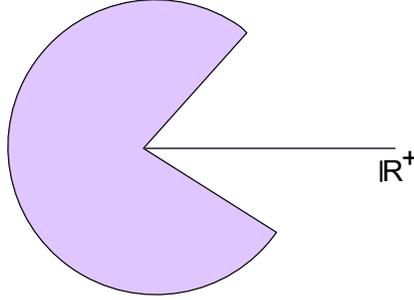


Figure 9: Type of sectors in $\epsilon$-space in Shishikura's paper

It uses the construction of Fatou coordinates embedding $f_\epsilon$ into the time-one map of (2.4) by means of the Ahlfors-Bers theorem [25].

- We lift $f_\epsilon$ by means of

$$Z = \begin{cases} \frac{1}{2\sqrt{\epsilon}} \ln \frac{z - \sqrt{\epsilon}}{z + \sqrt{\epsilon}} & \epsilon \neq 0 \\ -\frac{1}{z} & \epsilon = 0. \end{cases} \tag{2.13}$$

  The image of $U \setminus \{\pm\sqrt{\epsilon}\}$ is $\hat{U}$, which is $C \setminus B_0$ (resp. $C \setminus \cup_{k \in Z} B_k$) where the $B_k$ are disjoint simply connected domains of $C$. $B_0$ contains the origin and is called the *fundamental hole*.

- This change of coordinates has the property of transforming the diffeomophism $f_\epsilon$ to a small perturbation of the translation by 1. Namely $f_\epsilon(z)$ becomes

$$F_\epsilon(Z) = Z + 1 + R(\epsilon, Z), \tag{2.14}$$

  with $R(\epsilon, Z)$ and $\frac{\partial}{\partial Z} R(\epsilon, Z)$ small.

- We consider *admissible lines l*, which are lines such that $\ell$ and $F_\epsilon(\ell)$ generate fundamental domains $\hat{C}_\epsilon$ for $F_\epsilon$ (Figure 10).

- Families of admissible lines can be chosen depending continuously on $\hat{\epsilon} \in V_\delta$ (and analytically of $\hat{\epsilon} \neq 0$) as in Figure 11.

- The admissible lines generate *translation domains $Q(\ell)$*:

$$Q(\ell) = \{Z | \exists n \in Z,\ F_\epsilon^n(Z) \in \hat{C}_\epsilon \text{ and } \forall m \in [0, n] F_\epsilon^m \in \hat{U}\}. \tag{2.15}$$

  Remark that a translation domain is independent of the admissible line which generates it, as long as the admissible line is deformed within $\hat{U}$ while remaining admissible.
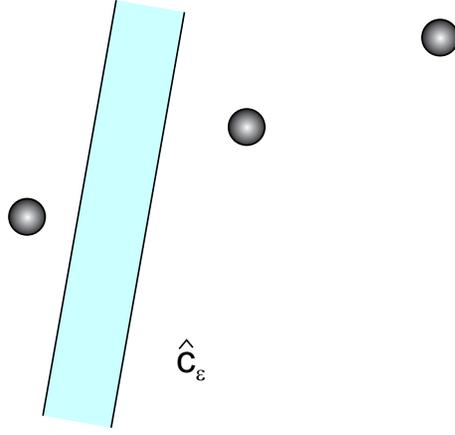
12

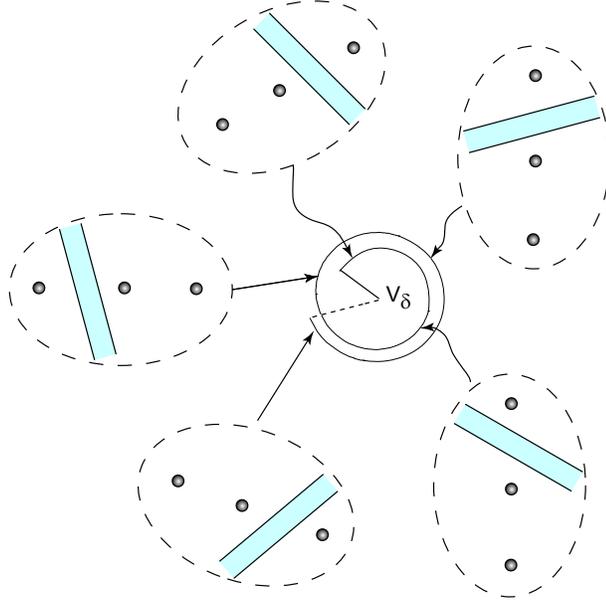Figure 10: A fundamental domain generated by an admissible line



Figure 11: Admissible lines depending continuously on $\hat{\epsilon}$

- On a translation domain $Q$ we construct a Fatou coordinate $\Psi_\epsilon$ conjugating $F_\epsilon$ with $Z \mapsto Z + 1$:

$$\Phi_\epsilon(F_\epsilon(Z)) = \Phi_\epsilon(Z) + 1. \tag{2.16}$$

Fatou coordinates are holomorphic diffeomorphisms. Moreover they are uniquely defined up to a translation.

The construction is done in two steps

i) We first construct in a very rough way a homeomorphism $h : Q \to C$ conjugating $F_\epsilon$ with $Z \mapsto Z + 1$. If $\ell = \{Z_1 + Ye^{i\theta} | Y \in R\}$, then

$$h^{-1}(X, Y) = (1 - X)(Z_1 + Ye^{i\theta}) + XF_\epsilon(Z_1 + Ye^{i\theta}). \tag{2.17}$$

ii) The mapping $h^{-1}$ is quasi-conformal. Indeed let

$$\mu = \frac{\partial h^{-1}/\partial \overline{Z}}{\partial h^{-1}/\partial Z}. \tag{2.18}$$

13

We extend $\mu$ in a periodic way to all of $C$ by the translation $Z \mapsto Z + 1$. The map $\mu$ is in $L^{\infty}(C)$ and has $L^{\infty}$-norm $||\mu||_{\infty} < 1$. So $\mu$ is a Beltrami field. It induces $\tilde{\mu}$ on $S^2$ by means of $Z \mapsto \exp(-2\pi i Z)$ and we let $\tilde{\mu}(0) = \tilde{\mu}(\infty) = 0$.

By Ahlfors-Bers measurable mapping theorem, if $\mu_0$ is the standard conformal structure on $S^2$, then

$$\exists! \tilde{h}_1 : S^2 \to S^2 \tag{2.19}$$

such that

$$\begin{cases} \tilde{h}_1^* \mu_0 = \tilde{\mu} \\ \tilde{h}_1(0) = 0 \\ \tilde{h}_1(\infty) = \infty \\ \tilde{h}_1(1) = 1. \end{cases} \tag{2.20}$$

We lift $\tilde{h}_1$ to $h_1$ such that $h_1(0) = 0$ and $h_1(1) = 1$. Then

$$\Phi = h_1 \circ h \tag{2.21}$$

is quasi-conformal and preserves the standard conformal structure. Hence $\Phi$ is conformal and conjugates $F_\epsilon$ with $Z \mapsto Z + 1$.

- If we choose a base point $Z_0(\epsilon)$ depending holomorphically on $\epsilon$, then the unique Fatou coordinate satisfying $\Phi_\epsilon(Z_0(\epsilon)) = 0$ depends continuously on $\hat{\epsilon}$ near $\hat{\epsilon} = 0$ and holomorphically on $\hat{\epsilon} \neq 0$.

$\square$

There exists two different ways of constructing the modulus:

I. We take two Fatou coordinates $\Phi_\epsilon^{\pm}$ associated to two admissible lines passing between holes and located on the two sides of the fundamental hole (Figure 12).
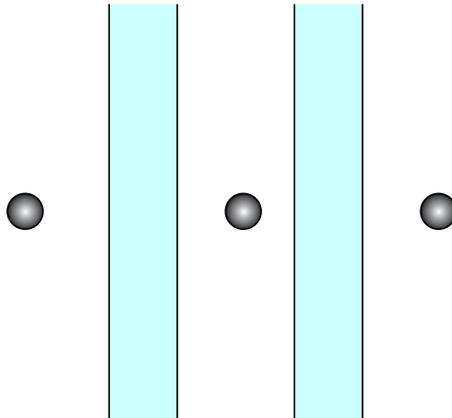


Figure 12: Two fundamental domains on each side of the fundamental hole

The modulus is defined as

$$\Psi_\epsilon = \Phi_\epsilon^+ \circ (\Phi_\epsilon^-)^{-1}. \tag{2.22}$$

It is defined on a domain as in Figure 13.

Using $Z \mapsto \exp(-2\pi i Z)$ this yields the two diffeomorphisms $\psi_\epsilon^\infty$ and $\psi_\epsilon^0$ of Figure 8, which are the unfolding of the Ecalle-Voronin modulus.
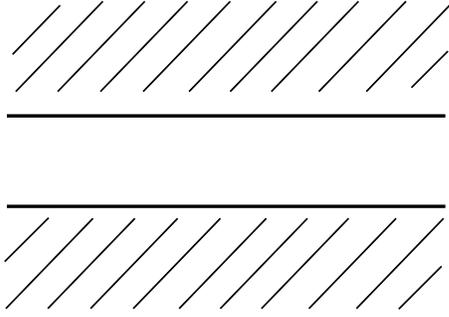
14

Figure 13: The domain of the modulus $\Psi_\epsilon$

II. The second method does not pass to the limit when $\epsilon \to 0$ but it allows to study the dynamics of $\sqrt{\epsilon}$. Indeed we have a global transition diffeomorphism, called the *Lavaurs map*

$$L_\epsilon : S_\epsilon^- \to S_\epsilon^+ \tag{2.23}$$

sending a point $w \in S_\epsilon^-$ to the first point of $S_\epsilon^+$ belonging to the orbit of $w$ under $f_\epsilon$ when iterating $f_\epsilon$ positively. As the Lavaurs map is global and sends 0 to 0 and $\infty$ to $\infty$ it is linear:

$$w \mapsto L_\epsilon(w) = \tau(\epsilon)w \tag{2.24}$$

with $\tau(\epsilon) \neq 0$. This second point of view allows to define *renormalized return maps* and to describe the *parametric resurgence*.

**The renormalized return maps.** They are defined as
$k_\epsilon^\infty, k_\epsilon^0 : S_\epsilon^+ \to S_\epsilon^+$ (Figure 14) as:

$$\begin{array}{rcl} k_\epsilon^\infty(w) & = & \tau(\epsilon)\psi_\epsilon^\infty(w) \\ k_\epsilon^0(w) & = & \tau(\epsilon)\psi_\epsilon^0(w). \end{array} \tag{2.25}$$
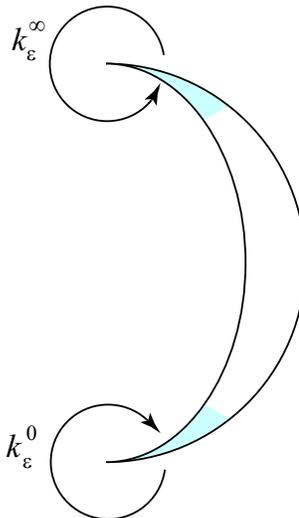


Figure 14: The return maps on $S_\epsilon^+$

15

The derivatives of $k_\epsilon^\infty$ at $\infty$ (resp. $k_\epsilon^0$ at 0) are analytic invariants:

$$
\begin{aligned}
k_\epsilon^{0'}(0) &= \exp(4\pi^2/\mu_-) \\
\tilde{k}_\epsilon^{\infty'}(0) &= \exp(4\pi^2/\mu_+),
\end{aligned}
\tag{2.26}
$$

where $\tilde{k}^\infty$ is the expression of $k^\infty$ in the coordinate $1/w$. (Note that $\infty$ (resp. 0) corresponds to $\sqrt{\epsilon}$ (resp. $-\sqrt{\epsilon}$) and .

**The parametric resurgence.**

We will limit ourselves to describe the parametric resurgence at $-\sqrt{\epsilon}$ by means of $\psi_\epsilon^0$. Let us first remark that it is possible to choose coordinates on $S_\epsilon^+$ and $S_\epsilon^-$ so that

$$
\psi_\epsilon^0(w) = w + \sum_{n>1} b_n(\epsilon) w^n,
\tag{2.27}
$$

with the $b_n(\epsilon)$ depending continuously on $\epsilon$. In particular for $\epsilon = 0$

$$
\psi^0(w) = w + \sum_{n>1} b_n w^n,
\tag{2.28}
$$

where $b_n = b_n(0)$, is half of the Ecalle-Voronin modulus. Hence if $\psi^0$ is nonlinear, then $\psi_\epsilon^0$ is nonlinear for all small $\epsilon$.

**The particular case where $\lambda_- = \exp(\mu_-) = \exp\left(-\frac{2\pi i}{n}\right)$, with $n$ large.** Then

$$
k_\epsilon^{0'}(0) = 1.
\tag{2.29}
$$

Hence $k_\epsilon^0$ nonlinear implies that $k_\epsilon^0$ non linearizable.

**The general case.** We consider the resonances

$$
\lambda_- = \exp(\mu_-) = \exp\left(-\frac{2\pi i p}{n}\right), \qquad n \equiv q \ (\text{mod } p)
\tag{2.30}
$$

with $n$ large. Then

$$
k_\epsilon^{0'}(0) = \exp\left(2\pi i \frac{q}{p}\right).
\tag{2.31}
$$

**2.3 Theorem** *[27]* If

$$
g(w) = \exp\left(2\pi i \frac{q}{p}\right) \psi^0(w)
\tag{2.32}
$$

*is nonlinearizable, then $k_\epsilon^0$ is non linearizable for $\epsilon$ such that*

$$
\begin{cases}
\lambda_- = \exp\left(-2\pi i \frac{p}{n}\right) \\
n \ large \\
n \equiv q \ (mod \ p).
\end{cases}
\tag{2.33}
$$

*This occurs as soon as one of the coefficients of the normal form of $g(w)$ does not vanish. The k-th coefficient of the normal form of $g(w)$ is a quasi-homogeneous polynomial*

$$
L_{p,q}^k(b_2, \ldots b_{kq+1}).
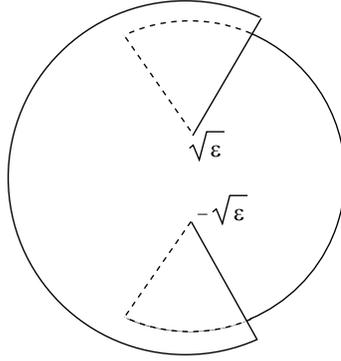\tag{2.34}
$$

16

Figure 15: The domain on which the diffeomorphism is embedded in the model

## 2.3 The two ways to normalize to the model

The Fatou coordinates allow us to find a normalizing transformation to the model.

**We have embedded the diffeomorphism into the model in the middle (between $\pm\sqrt{\epsilon}$) and read the incompatibility when turning around $\pm\sqrt{\epsilon}$:** we have found a change of coordinate transforming $f_\epsilon(z)$ to the model over a ramified neighborhood of $\pm\sqrt{\epsilon}$ for $\hat{\epsilon} \in V_\delta$ (Figure 15).

We compare this point of view with the Glutsyuk point of view [15] which was already introduced by Martinet [26].

Glutsyuk works for values of $\epsilon$ in a sector $V$

$$\begin{cases} |\epsilon| < r \\ \arg(\epsilon) \in (-\pi + \delta, \pi - \delta). \end{cases} \tag{2.35}$$

For any such $\epsilon \in V$, the diffeomorphism $f_\epsilon$ is linearizable in the neighborhood of $\pm\sqrt{\epsilon}$. Glutsyuk finds two changes of coordinates defined in neighborhoods of each singular point transforming $f_\epsilon(z)$ to the linear model in the neighborhood of $\pm\sqrt{\epsilon}$. He reads the incompatibility on the intersection of the two neighborhoods (Figure 16).
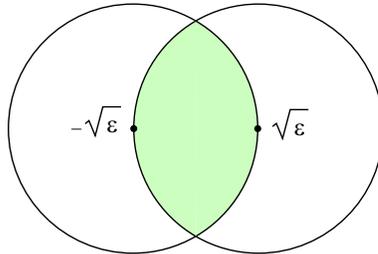


Figure 16: The fundamental domains in Glutsyuk point of view

Our method allows to recover Glutsyuk results. Indeed it suffices to take two admissible lines parallel to the lines of holes and located on each side of the line of holes (Figure 17).

They generate translation domains $Q^0$ and $Q^\infty$ on which we have Fatou coordinates $\Phi_\epsilon^0$ and $\Phi_\epsilon^\infty$. $\Phi_\epsilon^0$ and $\Phi_\epsilon^\infty$ are changes of coordinates transforming the diffeomorphism to the model diffeormorphism. As the model is linearizable near $\pm\sqrt{\epsilon}$ this is equivalent to find linearizing changes of coordinates. The *Glutsyuk modulus* is then given by

$$\Psi_\epsilon^G = \Phi_\epsilon^0 \circ (\Phi_\epsilon^\infty)^{-1}. \tag{2.36}$$

The Glutsyuk modulus is equivalent to the modulus $[(\psi_\epsilon^0, \psi_\epsilon^\infty)]$ described before (see [27]).
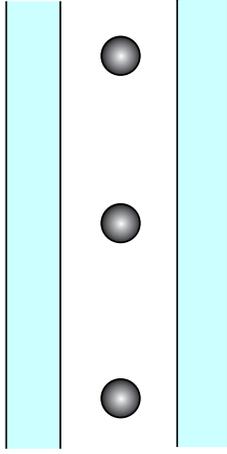
17

Figure 17: The admissible lines in Glutsyuk point of view

**In the Glutsyuk point of view we normalize near the singular points $\pm\sqrt{\epsilon}$ and read the incompatibility in the middle.**

# 3   Applications

One motivation for the previous study comes from work of the author with P. Mardešić and C. Christopher, [5] and [4]. In these papers we tried to understand how the strata of integrable and linearizable systems at the origin are organized in a family of polynomial systems

$$
\begin{array}{rcl}
\dot{x} & = & x + \sum_{i+j=2}^{n} a_{ij} x^i y^j \\
\dot{y} & = & -\lambda y + \sum_{i+j=2}^{n} b_{ij} x^i y^j
\end{array}
\tag{3.1}
$$

where $\lambda \in R^+$ and $a_{ij}, b_{ij} \in C$. We observed strange behaviours which we can now explain with the new tools developed in the previous section.

In [4] we study the family of Lotka-Volterra systems:

$$
\begin{array}{rcl}
\dot{x} & = & x(1 + ax + by) \\
\dot{y} & = & y(-\lambda + cx + dy)
\end{array}
\tag{3.2}
$$

where we want to identify all integrable systems for all $\lambda = \frac{p}{q} \in Q^+$. A characterization exists for all $\lambda = n/2$ and $\lambda = 2/n$, $n \in N$ ([14] and [17]). Also all Darboux integrable systems are known [3]. As the system is simple we could calculate saddle quantities for several values of $\lambda \in Q^+$ and come with the following conjecture:

**3.1 Conjecture** [4] The following two mechanisms are sufficient to describe all systems (3.2) with an integrable point at the origin:

i) The system has one extra invariant algebraic curve apart from the two axes. (Limit cases are possible when one of the axes or the equator is a multiple invariant algebraic curve). Such cases are classified in [3].

ii) The system is integrable by the "monodromy argument".

**The monodromy argument.** This argument deals with the monodromy group of one of the two axes which are the separatrices of the origin. Let us describe it on the $x$-axis. The system has three singular points on $y = 0$, namely $(0,0)$, $P_1 = (-1/a, 0)$ and $P_\infty$ which is the point at infinity.

18

- It is known that the origin is integrable if and only if its monodromy map $M_0$ is linearizable.

- $M_0$ is conjugate to $M_\infty^{-1} \circ M_1^{-1}$ where $M_1$ (resp. $M_\infty$) is the monodromy of $P_1$ (resp. $P_\infty$), see Figure 18.
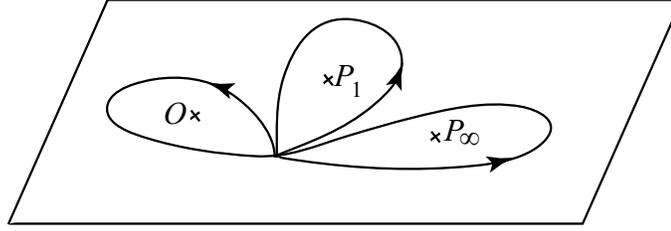


Figure 18: The monodromy group of the $x$-separatrix

- Hence a first sufficient condition for the linearizability of $M_0$ is given by $M_\infty \equiv id$ and $M_1$ linearizable. $M_\infty \equiv id$ as soon as it is a resonant node with eigenvalues $\mu_1, \mu_2$ with $\mu_2/\mu_1 \in N$ (we have no problem of resonance as the node has two analytic separatrices). Moreover $M_1$ is linearizable as soon as it is a non resonant node or a resonant node with a zero resonant monomial.

- Similarly a second sufficient condition for the linearizability of $M_0$ is given by $M_1 \equiv id$ and $M_\infty$ linearizable. This is realized if the eigenvalues $\nu_1, \nu_2$ of $P_1$ satisfy $\nu_2/\nu_1 \in N$ and $M_\infty$ linearizable. To realize $M_\infty$ linearizable we have two choices: either $P_\infty$ is a node (we have no problem of resonance as the node has two analytic separatrices) or it is a saddle and we play the monodromy argument on the line at infinity.

**3.2 Theorem** *[4] These two mechanisms are sufficient to provide necessary and sufficient conditions for integrability in the Lotka-Volterra system (3.2) for the following rational values of $\lambda$:*

- *$\lambda = n, 1/n$. This case was already studied in [14] but other arguments were used to prove that the conditions were necessary and sufficient.*

- *$\lambda = n/2, 2/n$. This case was already studied in [17] but other arguments were used to prove that the conditions were necessary and sufficient.*

- *$\lambda = \frac{p}{q}, p + q \leq 12$.*

The paper [4] also lists general conditions of integrability. One is the following:

**Condition (*).**
    The system (3.2) is integrable if

$$(*) \begin{cases} a = -c \\ \lambda > 1, \ \lambda \neq 1 + \frac{1}{m} \text{ with } m \in N. \end{cases} \tag{3.3}$$

If $\lambda = 1 + \frac{1}{m}$, an additional condition is necessary for integrability.

    Let us explain condition (*). The condition $a = -c$ guarantees that $P_\infty$ is a node with eigenvalues in the ratio $1 : 2$ yielding $M_\infty \equiv id$. The condition $\lambda > 1$ guarantees that $P_1$ is a node. If $\lambda \neq 1 + \frac{1}{m}$ the node is non resonant, yielding that $M_1$ is linearizable. If $\lambda = 1 + \frac{1}{m}$ then the node is resonant with eigenvalues in the ratio $n : 1$ and we need to ask that the resonant monomial has a zero coefficient.

19

In practice when $b, c \neq 0$ we can scale $b = c = 1$ yielding $a = -1$ and the family depends only on the parameter $d$:

$$\begin{aligned} \dot{x} &= x(1 - x + y) \\ \dot{y} &= x(-\lambda + x + dy). \end{aligned} \qquad (3.4)$$

Then condition (*) yields a stratum of dimension 1 (resp. strata of dimension 0) when $\lambda > 1$, $\lambda \neq 1 + 1/m$ (resp. $\lambda = 1 + 1/m$), see Figure 19. The pathological values $\lambda = 1 + 1/m$ accumulate to $\lambda = 1$. So the following questions are natural:

**Questions:**

(1) What happens for $\lambda = 1$? Indeed the integrable points for $\lambda = 1 + 1/m$ of Figure 19 show a nice pattern of sequences with accumulation points on $\lambda = 1$.

(2) What happens for $\lambda < 1$?
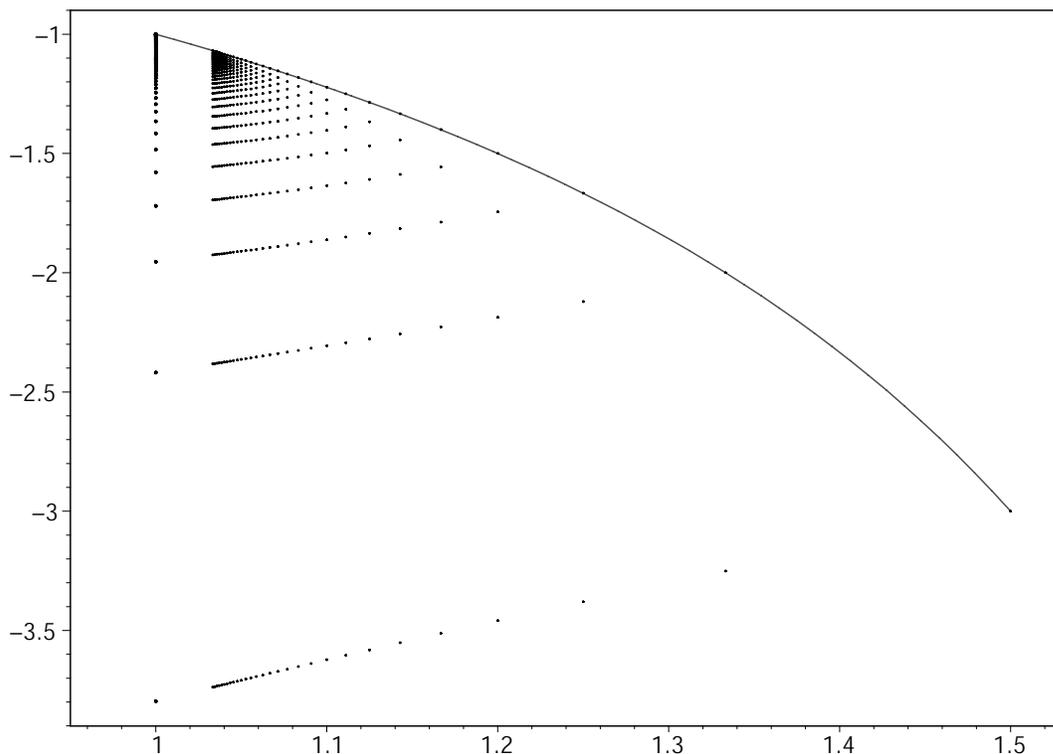


Figure 19: The values of $d$ for which the system (3.4) is integrable for $\lambda = 1 + 1/n$. The system is integrable on the curve $d = \frac{\lambda}{\lambda - 2}$.

**Computational answers:**

(1) Calculations yield that for $\lambda = 1$ the origin is integrable only if $d = -1$. So all limit points except one are not integrable.

(2) Calculations on the side $\lambda < 1$, in particular for $\lambda = 1 - 1/m$ show that points seem generically non integrable, so the pattern seems not to be symmetric.

**Explanation:** Except for $d = -1$ the map $M_0$ has a generic parabolic point as studied in the previous section. The limit points at $\lambda = 1$ in Figure 19 are *semi-normalizable*: If $(\psi^0, \psi^\infty)$ is the Ecalle-Voronin

20

modulus of $M_0$, then we have

$$\begin{cases} \psi^\infty \text{ linear} \\ \psi^0 \text{ non linear.} \end{cases} \tag{3.5}$$

At $\lambda = 1$ we have a *transcritical bifurcation*. Indeed $M_0$ has two fixed points for $\lambda \neq 1$ and a double fixed point for $\lambda = 1$. The first fixed point is the origin and the second fixed point corresponds to an invariant manifold [22]. These two points "pass through each other" at $\lambda = 1$ as is usual in a transcritical bifurcation (Figure 20):

- For $\lambda < 1$, $\psi^\infty$ controls the invariant manifold while $\psi^0$ controls the origin. Hence the origin is necessarily non trivial by Theorem 2.3 for $\lambda = 1 - 1/m$ with $m$ large, while the invariant manifold may or may not be trivial.

- For $\lambda > 1$, $\psi^\infty$ controls the origin which can hence be integrable if $d(\lambda)$ is well chosen, while $\psi^0$ controls the invariant manifold which is necessarily nontrivial for $\lambda = 1 + 1/m$ by Theorem 2.3.
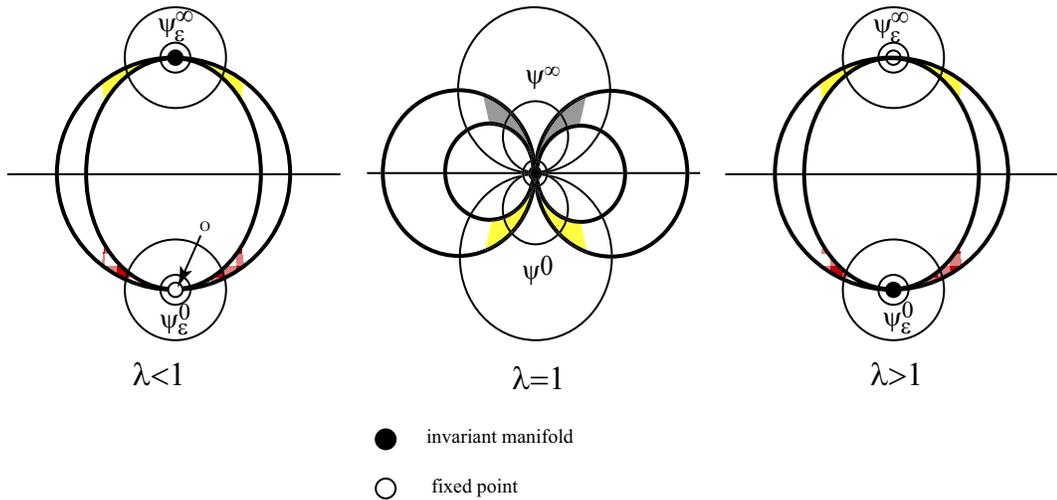


Figure 20: The transcritical bifurcation

**Other consequence:** For $\lambda = 1$ we can say more about the points which are not limit points of sequences of integrable systems for $\lambda = 1 + 1/m$. These points are approached by integrable saddles as soon as $\lambda \neq 1 + 1/m$. If $(\psi^0, \psi^\infty)$ is the Ecalle-Voronin modulus of the limit point, then we know that the unfolding $\psi^\infty$ controls the origin for $\lambda > 1$. Hence necessarily $\psi^\infty$ is a Möbius function by Theorem 1.1.

# 4    The finiteness part of Hilbert's 16th problem for quadratic systems

Hilbert's 16th problem asks for the maximum number $H(n)$ of limit cycles of a polynomial planar vector field of degree $\leq n$. It is still open for any $n$. Since the simultaneous proofs of Ecalle and Ilyashenko in 1987 it is known that a single vector field has a fnite number of limit cycles. The finiteness part of Hilbert's 16th problem deals with the existence of a uniform bound for the number of limit cycles of a polynomial system of degree $\leq n$:

**The finiteness part of Hilbert's problem for polynomial vector fields.** $\forall n \in N \ \exists M(n) \in N$ such that any polynomial vector field

$$\begin{aligned} \dot{x} &= P(x, y) \\ \dot{y} &= Q(x, y) \end{aligned} \tag{4.1}$$

21

with $P, Q, \in R[x, y]$ and $\max(\deg(P), \deg(Q)) \leq n$ has at most $M(n)$ limit cycles. It is usually given in the condensed form

$$H(n) < \infty. \tag{4.2}$$

In [9] a strategy was developed to attack the finiteness part in the particular case $n = 2$. The idea of the strategy is the following. It is possible to compactify the phase space to the Poincaré sphere. Hence, if there is an infinite number of limit cycles then they need to accumulate on some graphics. This idea is sufficient to prove that any individual polynomial vector field has a finite number of limit cycles. For quadratic systems the proof is elementary [2]. Moreover the coefficients of the system are parameters. Rescaling time it is possible to consider the parameter space of nonzero vector fields of degree $\leq 2$ as a compact space. Limit cycles depend on the parameters and accumulate on "limit periodic sets", which we want to look at as "local" objects. If all these limit periodic sets have *finite cyclicity*, a "local finiteness property", then we can expect a uniform bound for the number of limit cycles.

**Notation for the figures:** In all this section double arrows on an invariant manifold in the figures indicate hyperbolicity in that direction, i.e. the corresponding eigenvalue is nonzero.

**4.1 Definition** A limit periodic set $\Gamma$ of a vector field $v_{\lambda_0}$ has *finite cyclicity inside a family of vector fields* $\{v_\lambda\}_{\lambda \in \Lambda}$ if $\exists \epsilon > 0, \delta > 0, \exists N \in N$ such that any $v_\lambda$ with $|\lambda - \lambda_0| < \delta$ has at most $N$ limit cycles $\gamma_1, \ldots \gamma_m$ such that $d_H(\gamma_i, \Gamma) < \epsilon$, where $d_H$ is the Hausdorff distance between compact sets.

**4.2 Theorem** *[9]*

$$H(2) < \infty. \tag{4.3}$$

*if and only if all 121 limit periodic sets surrounding the origin in the family*

$$\begin{aligned}
\dot{x} &= \lambda x - \mu y + a_1 x^2 + a_2 xy + a_3 y^2 \\
\dot{y} &= \mu x + \lambda y + b_1 x^2 + b_2 xy + b_3 y^2,
\end{aligned} \tag{4.4}$$

$(\lambda, \mu) \in S^1$, $(a_1, a_2, a_3, b_1, b_2, b_3) \in S^5$ *have finite cyclicity inside the family* (4.4).

Although the paper [9] was published in 1994, the program is started since 1991. It progresses well. The purpose of the present section is to present its actual status with a discussion on what is done and what remains to be done. Since 1994 no error was found in the list of graphics of [9]. The author however feels that the list should have contained 125 graphics. Indeed the list of [9] is a list up to topological equivalence. Four graphics with elliptic point appear in two forms (Figure 21) which in the blow-up are not topologically equivalent. The graphics appear in Figure 22.

The Table 1 lists the different classes of graphics and what is done in each case.
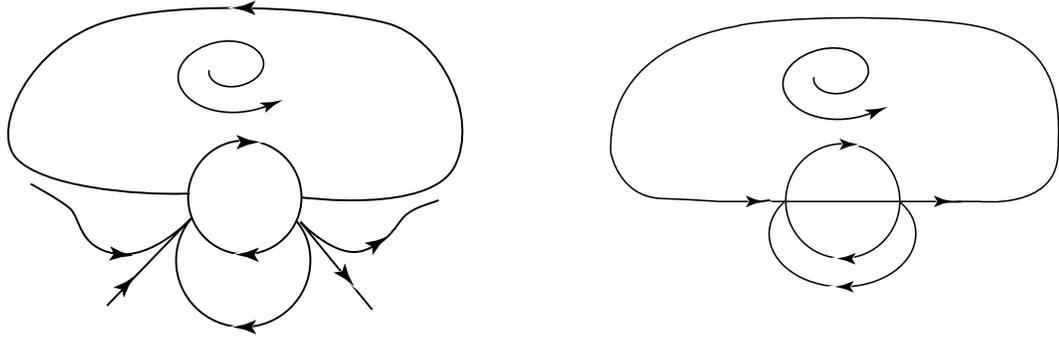
22

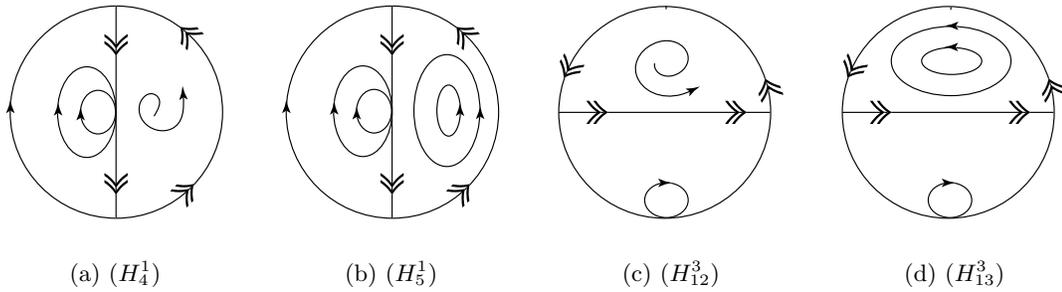Figure 21: The two forms of an hh-graphic through an elliptic point



(a) $(H_4^1)$      (b) $(H_5^1)$      (c) $(H_{12}^3)$      (d) $(H_{13}^3)$

Figure 22: The 4 additional cases

| Class of graphics | Done | Open but probably easy | Open |
|---|---|---|---|
| Hyperbolic graphics | 10 (Mourtada) | | |
| Elementary non hyperbolic graphics | 47 | 1 | |
| Graphics through a nilpotent saddle | 2 | | 2 (center cases) |
| Graphics through a nilpotent elliptic point with pp-transition | 16 | | 4 (center cases) |
| Graphics through a nilpotent elliptic point with hp-transition | 6 | 4 | |
| Graphics through a nilpotent elliptic point with hh-transition (mult. 3) | 2 | 4 | 6 (center cases |
| The four additional cases | | | 4 |
| Graphics through a nilpotent elliptic point with multiplicity 4 | | | 4 |
| Degenerate graphics | | | 13 |
| Total = 125 | 83 | 9 | 33 |

Table 1

The different classes will be discussed below together with references for proofs. The category "open but probably easy" is obviously subjective and reflects the belief of the author that no new methods but merely elementary calculations can allow to prove finite cyclicity. The calculations may not be short. The

author has not checked all proofs. It is premature at this stage of the program, if we consider the fact that unifying proofs of many cases could appear before the program is completed.

**Strategies to attack the program and avoid making mistakes.**

(1) Start from the most generic graphics and follow with the more degenerate. As degenerate graphics bifurcate into generic graphics everything has to be coherent.

(2) Some graphics appear in families: the strategy is to study simultaneously all graphics in a family including the bordering graphics. Everything has to be coherent. Examples will be discussed below.

## 4.1   Hyperbolic graphics

Nearly all cases have been done, one by one, by elementary methods. More recently Mourtada announced

**4.3 Theorem** *([30], [31], [32], [33]) Any hyperbolic polycycle has finite cyclicity inside any analytic finite-parameter family of vector fields.*

When working with elementary methods the center cases are usually difficult problems. For instance the "triangle" (Figure 23) can lie at the intersection of 3 strata: indeed it has 3 invariant lines, yielding Darboux integrability. It can be time-reversible when there is a symmetry axis and it can simultaneously be Hamiltonian.
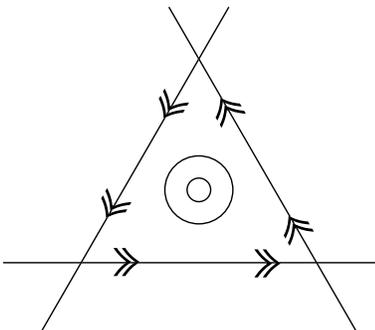


Figure 23: The triangle

## 4.2   Elementary non-hyperbolic graphics

**4.4 Definition** A graphic is *elementary* if all its singular points are *elementary* (i.e. with one or 2 nonzero eigenvalues), either hyperbolic saddles or *semi-hyperbolic points* (i.e. points with exactly one zero eigenvalue).

The finite cyclicity of these graphics are usually easier problems and all graphics are treated with elementary methods.

- The case $(I_{13}^2)$ is treated in [41].

- 46 cases are treated in different papers to which the author contributed: [10], [6], [7], [35].

- the graphic $(I_{16a}^2)$ is still open.

**Ingredients used.**

(1) $C^k$ normal forms near the saddle-nodes

$$\begin{aligned}
\dot{x} &= x^2 + \epsilon \\
\dot{y} &= \pm y(1 + ax)
\end{aligned} \tag{4.5}$$

and semi-hyperbolic saddles

$$\begin{aligned}
\dot{x} &= x^3 + \epsilon_2 x + \epsilon_1 \\
\dot{y} &= -y(1 + ax^2).
\end{aligned} \tag{4.6}$$

It is remarkable that the $C^k$ normal forms have been sufficient even in the center cases!

(2) We have two types of transition maps near a semi-hyerbolic point:

- **Central transition** (Figure 24a). The Dulac map is linear when it exists (it does not exist for $\epsilon = 0$!):
$$D_\epsilon(y) = m(\epsilon)y, \qquad \lim_{\epsilon \to 0} m(\epsilon) = 0. \tag{4.7}$$

- **Stable-center transition** (Figure 24b). The Dulac map $D_\epsilon$ is flat in $(x, \epsilon)$ and has additional flatness properties [10].



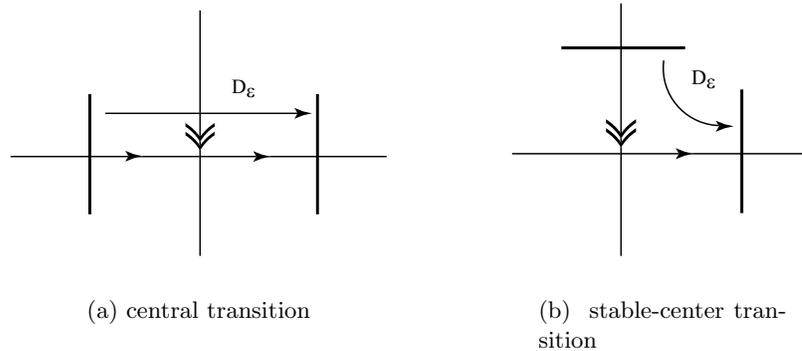(a) central transition          (b) stable-center transition

Figure 24: The Dulac maps for a saddle-node

(3) Khovanskii's method is used as soon as the Poincaré return map contains the composition of a stable-center transition with a center-unstable transition. The principle of *Khovanskii's method* is that the Dulac map is a solution of a Pfaff equation:

- **Case of a central transition.** The Pfaff equation is:
$$x\,dy - y\,dx = 0. \tag{4.8}$$

- **Case of a stable-center (center-unstable) transition.** The Pfaff equation is:
$$F(x)\,dy \mp y\,dx = 0, \tag{4.9}$$

where the normal form is

$$\begin{aligned}
\dot{x} &= F(x) \\
\dot{y} &= \mp y
\end{aligned} \tag{4.10}$$

25

(4) Except for $(I_{13}^2)$ which is treated in [41] all center cases are not located at the intersection of strata of centers: the *Bautin ideal* is radical allowing an elementary treatment [35].

Hence:

- we first make a proof in the generic case (e.g. $(I_4^2)$, Figure 25a);
- we then transform it into a proof for the center case by a Bautin type argument (e.g. $(I_5^2)$, Figure 25b).
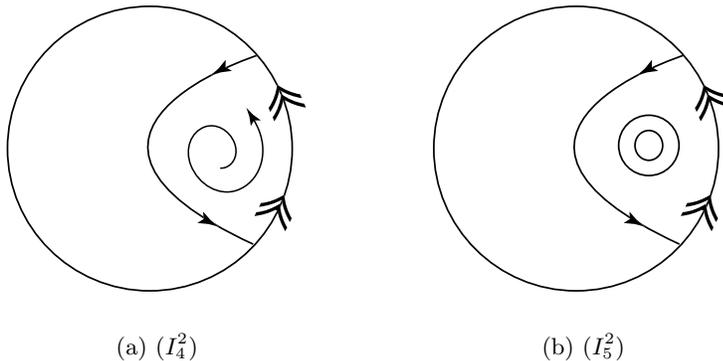


(a) $(I_4^2)$        (b) $(I_5^2)$

Figure 25: The graphics $(I_4^2)$ and $(I_5^2)$

**The left open case** $(I_{16a}^2)$**.** There is a continuum of graphics $(I_{16a}^2)$ (Figure 26): they occur inside a family.
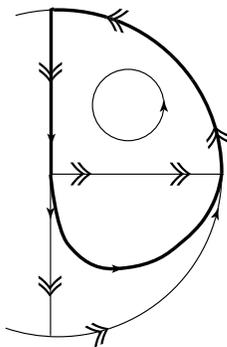


Figure 26: The graphic $(I_{16a})$

The bordering graphic $(I_{16b}^2)$ is treated in [35] and $(H_6^3)$ is treated in [7]. Moreover a proof of finite cyclicity is given in [7] for the corresponding generic graphics $(I_{14a}^2)$ and $(I_{15a}^2)$ appearing when breaking the center condition. As the Bautin ideal is radical we "should" be able, with mere calculations, to reduce the center case to the generic case via a Bautin type argument.

We still believe that such calculations can be done, but that they will take more than one or two pages.

**A remark on the genericity condition used to make the proof in the generic cases.** Note that any of the graphics $(I_{14a}^2)$, $(I_{15a}^2)$ and $(I_{16a}^2)$ is of the form appearing in Figure 27. We take sections near the singular points as in Figure 27 and calculate the different Dulac maps in the neighborhood of the singular points and regular transitions.
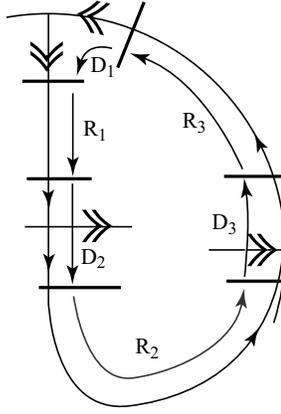
26

Figure 27: The transition maps for $(I^2_{14a})$, $(I^2_{15a})$ and $(I^2_{16a})$

The sections are taken in normalizing $C^k$ normal forms in the neighborhood of the singular points allowing an explicit calculation of the Dulac maps. In all the discussion $\lambda$ is the multi-parameter of the problem and we suppose that the graphic occurs at $\lambda = 0$. We discuss the easier case, namely the one where the hyperbolicity ratio at $P_1$ is $r(0)$, with $r(0)$ irrational (the other cases are similar but a little longer to write). Then the normal form near $P_1$ is

$$\begin{aligned} \dot{x}_1 &= x_1 \\ \dot{y}_1 &= -r(\lambda)y_1. \end{aligned} \tag{4.11}$$

Moreover we have

$$D_2(x_2) = M(\lambda)x_2, \qquad \lim_{\lambda \to 0} M(\lambda) = +\infty, \tag{4.12}$$

$$D_3(x_3) = m(\lambda)x_3, \qquad \lim_{\lambda \to 0} m(\lambda) = 0. \tag{4.13}$$

It is shown in [16] that the $C^k$-changes of coordinates to normal form are not unique. Using this freedom allows to simplify the regular transitions. Because the connection along the equator is fixed we can suppose that $R_3$ is the identity and $R_1(y_1) = y_1 + \delta$ is a translation. Hence the Poincaré return map is identically zero for some $\lambda$ if

$$R_{2,\lambda}(x_3) = \left[ m(\lambda)^{-1/r(\lambda)} M(\lambda)^{-1} x_3 - \delta \right]^{1/r(\lambda)}, \tag{4.14}$$

i.e. $R_{2,\lambda}$ is the $1/r$-th power of an affine map. A generic condition on $R_{2,0}$ for $\lambda = 0$ is that $R_{2,0}$ is not the $1/r$-th power of an affine map at the level of a finite jet.

**How to check this condition in practice?** A simple method, *the analytic extension principle,* exists because we deal with analytic vector fields. Indeed our graphic occurs in a family of graphics. Let us look near the boundary graphic which is the hemicycle (Figure 28). The transition maps $f$ and $g$ along the invariant line and the equator are nonlinear as soon as the hyperbolicity ratio of the point $P_4$ is different from 1.

Indeed in [7] we showed through an explicit calculation that $f$ and $g$ have a non-vanishing second derivative. In the particular case where the hyperbolicity ratio is equal to 1 it is possible to prove that $P_4$ is non-integrable (the first saddle quantity is nonzero).

- So graphics very close to the hemicycle verify the genericity condition.

- The analycity extension principle guarantees that we can choose the sections $\Pi_2$ and $\Sigma_3$ analytic and parametrized by analytic coordinates. Hence we can "push" the genericity condition to the whole family of graphics.
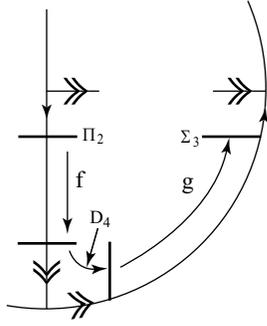
Figure 28: The lower part of the hemicycle

The analycity extension principle lies on the following theorems proved in [8].

**4.5 Theorem** *A saddle-node of an analytic vector field can be brought in the neighborhood of the origin to the normal form*

$$\begin{aligned} \dot{x} &= x^2 \\ \dot{y} &= \pm y(1 + ax) \end{aligned} \tag{4.15}$$

*by a $C^\infty$ change of coordinates which is analytic outside $x = 0$.*

**4.6 Theorem** *For a $C^\infty$ unfolding of a germ of analytic vector field with a saddle-node at the origin there exists a finitely smooth orbital equivalence with the polynomial normal form*

$$\begin{aligned} \dot{x} &= x^2 - \epsilon \\ \dot{y} &= \pm y(1 + ax). \end{aligned} \tag{4.16}$$

*For $\epsilon = 0$ this equivalence is analytic outside the strong manifold.*

## 4.3   Graphics through a nilpotent saddle

**4.7 Theorem** *(Zhu [40]) A "convex" graphic through a nilpotent saddle of codimension 3 (Figure 29) has finite cyclicity if the return map has a derivative different from 1.*
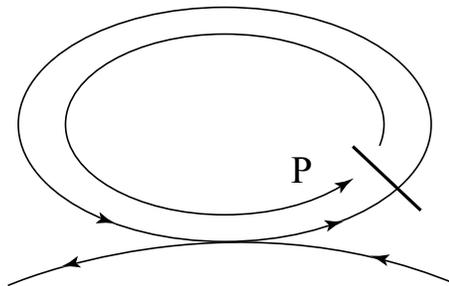


Figure 29: A "convex" graphic through a nilpotent saddle

The two cases appearing in Figure 30 have been shown to have finite cyclicity:

28

- the transition occurs along an invariant parabola allowing to calculate $P'(0)$.

- A few adjustments to the proof allow to treat the case with an additional saddle-node.

- The point can be of codimension 4, but the transition is fixed along the equator so the proof of the theorem 4.7 can be easily adjusted to this case.
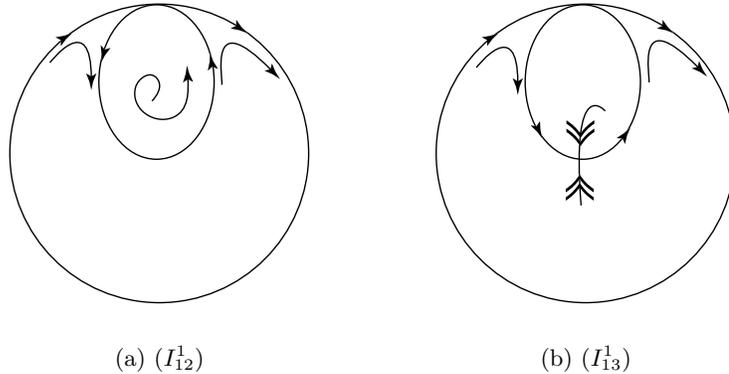


(a) $(I_{12}^1)$                    (b) $(I_{13}^1)$

Figure 30: The two graphics with nilpotent saddle and finite cyclicity

The two cases which remain to be done are two center cases. Moreover they can lie at the intersection of strata of centers.

## 4.4  The 3 types of transition through an elliptic nilpotent point of multiplicity 3

They appear in Figure 31: on the left we draw the graphics. On the right the same graphics are drawn when the elliptic point has been blown up. They are called pp-graphic (resp. hp-graphic, hh-graphic) using the names of [23]. In the names "p" refers to a parabolic sector and "h" to a hyperbolic sector. Hence an hp graphic starts between two hyperbolic sectors to end in a parabolic sector.
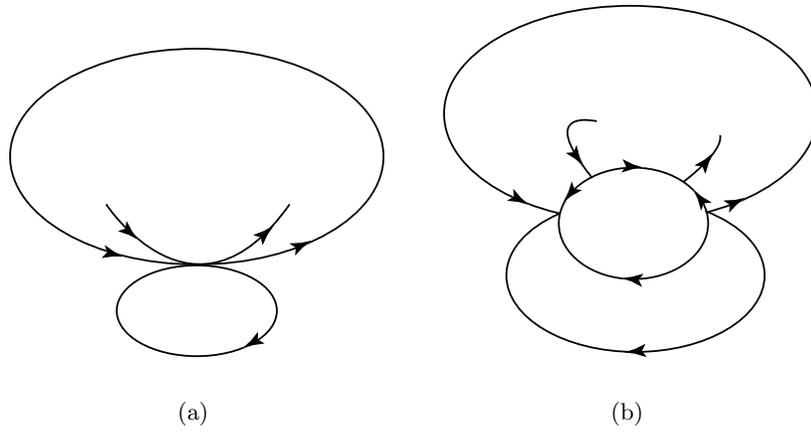
**4.8 Theorem** *(Zhu [40]) A graphic through a nilpotent elliptic point of multiplicity 3 has finite cyclicity under one of the following conditions:*

- **hp-graphic***: no condition;*

- **pp-graphic***: the transition map in normal coordinates near the singular points on the blow-up circle (Figure* 32*) is nonlinear;*

- **hh-graphic***: the point is of codimension 3 and the return map has a derivative different from 1.*
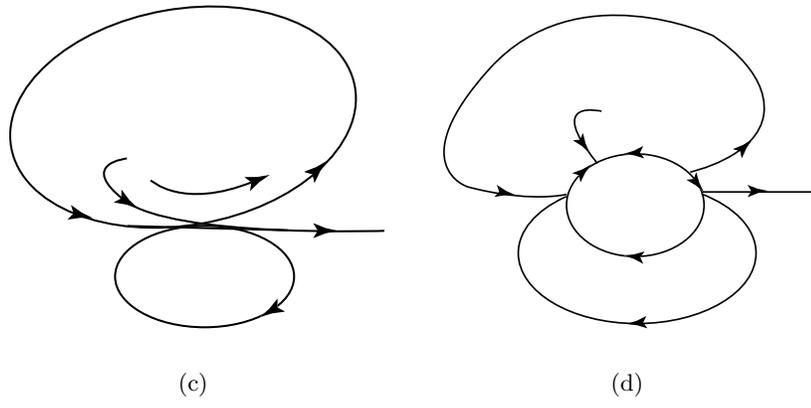
We will discuss the fact that the hypotheses which look so different for the 3 cases are indeed consistent.
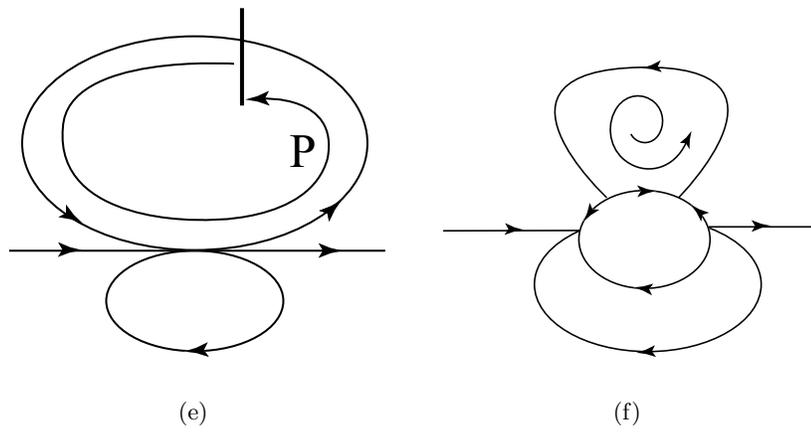
**Consistency of the hypotheses.**

- An hp-graphic contains pp-graphics in its neighborhood and can bifurcate into a pp-graphic. All these pp-graphics satisfy the genericity condition. This comes from the nonlinearity of the passage from $\Sigma$ to $\Pi$ in Figure 33.

(a)                                          (b)

pp-graphic



(c)                                          (d)

hp-graphic



P

(e)                                          (f)

hh-graphic

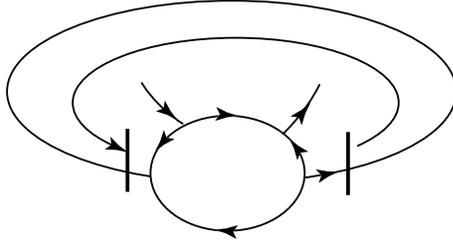Figure 31:   The three types of graphics through an elliptic point
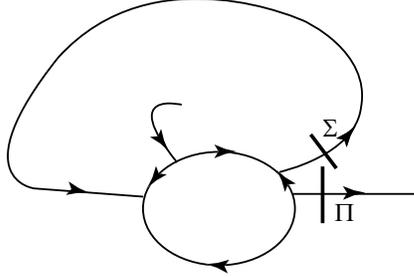
30

Figure 32: A pp-graphic



Figure 33: Nonlinearity of the passage from $\Sigma$ to $\Pi$

- Similarly an hh-graphic can bifurcate into hp- and pp-graphics. The pp-graphics produced are generic because the two passages from $\Sigma_i$ to $\Pi_i$ in Figure 34 are nonlinear and nearly symmetric one to the other. The transition map from $\Pi_2$ to $\Pi_1$ remains nonlinear (there is no compensation) as $P'(0) \neq 1$.

**What remains to be done for quadratic systems?** Essentially to adapt the proof of Theorem 4.8 when either the nilpotent point is of multiplicity four or there are additional singular points on the graphics: up to two hyperbolic saddles and/or one saddle-node. Also all center cases need to be done.

**Case of pp-graphics**

- All adaptations have been done in [36] for the graphics with extra singular points and not surrounding a center.

- Four center cases remain to be done.

**Case of hp-graphics**

- Adaptations to the graphics with an extra saddle-node have been done.

- Adaptations to the graphics with an extra saddle remain to be done. If the saddles have had a hyperbolicity ratio $r < 1$ the adaptation would have been a few lines. In quadratic systems we always have the bad case $r > 1$. We still hope to solve the 4 remaining cases with mere calculations.

**Case of hh-graphics**

- As for graphics through a nilpotent saddle, the transition occurs along an invariant parabola, allowing to calculate $P'(0)$.
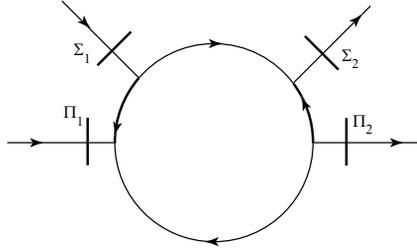
31

Figure 34: The passage from $\Sigma_i$ to $\Pi_i$

- An adaptation is needed for the codimension 4 case. The codimension 4 type I corresponds to $\epsilon = 0$, $b > 2\sqrt{2}$, in the normal form

$$
\begin{aligned}
\dot{x} &= y \\
\dot{y} &= -x^3 + bxy + \epsilon x^2 y + o(|x, y|^5).
\end{aligned}
\tag{4.17}
$$

The condition $\epsilon \neq 0$ was used to show that the transition maps of Figure 35 are nonlinear.
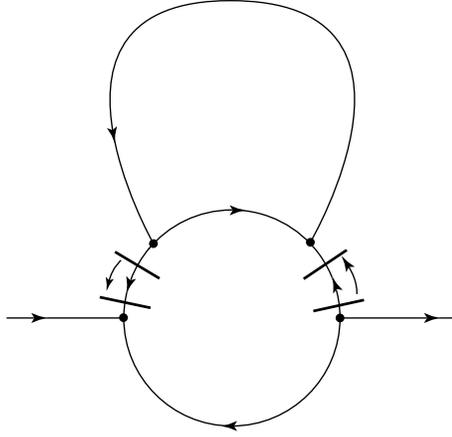


Figure 35: The two transition maps along arcs of the blow-up circle

For quadratic systems with $\epsilon = 0$ the four singular points on the blow-up circle are non integrable as soon as $P'(0) \neq 1$, hence we believe that the proofs can be adapted.

- An adaptation is needed for hemicycles (2 extra saddles) (Figure 36) with the nilpotent point on the invariant line or at infinity. We may have an additional saddle-node.

- The center cases have to be done.

## 4.5 The four additional cases

These are four graphics with a nilpotent elliptic point of codimension 4 type II ($b = 2\sqrt{2}$ in (4.17)) (see Figure 37).

A priori we could expect to be able to treat the generic cases by the standard technique of the blow-up of the family.

As we work in quadratic systems and the nilpotent focus does not exist in quadratic systems (there is a fold in parameter space) we can take the following family as a normal form near the elliptic point

$$
\begin{aligned}
\dot{x} &= y + (\tfrac{1}{2} + \mu_4)x^2 + \mu_2 \\
\dot{y} &= \mu_1 + \mu_3 y + xy
\end{aligned}
\tag{4.18}
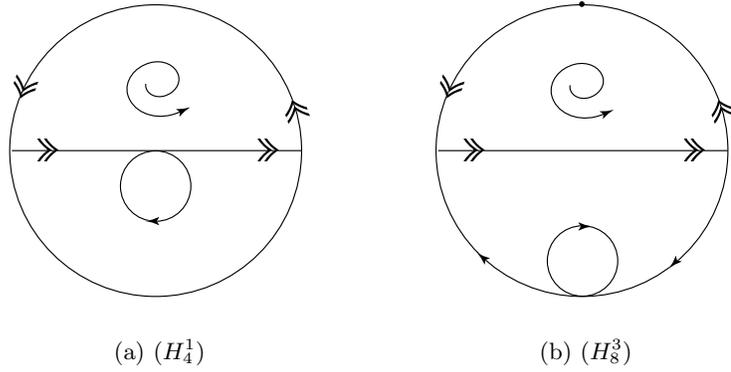$$

32

(a) $(H_4^1)$　　　　　　　　　　(b) $(H_8^3)$

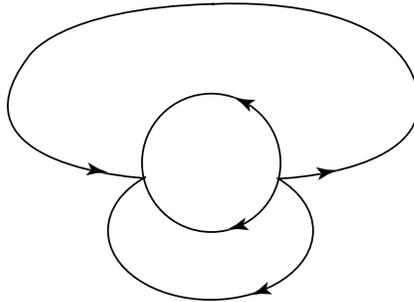Figure 36: The graphics $(H_4^1)$, $(H_8^3)$



Figure 37: The type of the 4 additional cases

The blow-up of the family is the following

$$
\begin{cases}
x = r\overline{x} \\
y = r^2\overline{y} \\
\mu_1 = r^3\rho^3\overline{\mu}_1 \\
\mu_2 = r^2\rho^2\overline{\mu}_2 \\
\mu_3 = r\rho\overline{\mu}_3,
\end{cases}
\tag{4.19}
$$

$(\overline{x}, \overline{y}, \rho) \in S^2$, $(\overline{\mu}_1, \overline{\mu}_2, \overline{\mu}_3) \in S^2$, $r, \mu_4$ small.

## 4.6  The graphics with a nilpotent point of multiplicity 4 and the degenerate graphics

Nilpotent points of multiplicity 4 have a normal form

$$
\begin{aligned}
\dot{x} &= y \\
\dot{y} &= x^4 + bxy + \ldots
\end{aligned}
\tag{4.20}
$$

Degenerate graphics have one or two lines of singular points.

A priori we expect that the method of the blow-up of the family adapted by Dumortier and Roussarie ([11] and [12]) for the Canard cycles can work for the generic cases. But the blow-up will generate lines of singular points in the blown-up family. So even for the graphics with a nilpotent point of multiplicity 4 we expect to apply the methods developed to study singular perturbations.

33

## 4.7 The status of all graphics

For the sake of completeness we have added the status of all graphics of the family. The names refer to the grahics of [9].

**Graphics done.**

- Hyperbolic graphics: $(F_1^1)$, $(F_2^1)$, $F_2^2$, $(F^3)$, $(H_1^1)$, $(H_2^1)$, $(I_1^2)$, $(I_2^2)$, $(I_6^2)$, $(I_7^2)$

- Semi-hyperbolic graphics: $(F_2^1)$, $(F_3^1)$, $(F_4^1)$, $(F_3^2)$, $(F_4^2)$, $(H_3^1)$, $(H_8^1)$, $(H_9^1)$, $(H_{10}^1)$, $(H_{11}^1)$, $(H_{12}^1)$, $(I_3^2)$, $(I_4^2)$, $(I_5^2)$, $I_8^2$, $(I_9^2)$, $(I_{10}^2)$, $(I_{11}^2)$, $(I_{12}^2)$, $(I_{13}^2)$, $(H_1^3)$, $(H_2^3)$, $(H_3^3)$, $(H_4^3)$, $(I_{14a}^2)$, $(I_{14b}^2)$, $(H_5^3)$, $(I_{15a}^2)$, $(I_{15b}^2)$, $(H_6^3)$, $(I_{16a}^2)$, $(I_{19}^2)$, $(I_{20}^2)$, $(I_{21}^2)$, $(I_{22}^2)$, $(I_{27}^2)$, $(I_{28}^2)$, $(I_{29}^2)$, $(I_{30}^2)$, $(I_{31}^2)$, $(I_{32}^2)$, $(I_{33}^2)$, $(I_{34}^2)$, $(I_{35}^2)$, $(I_{36}^2)$, $(I_{37}^2)$, $(I_{38}^2)$

- Graphics with a nilpotent saddle: $(I_{12}^1)$, $(I_{13}^1)$

- pp-graphics with a nilpotent elliptic point: $(H_6^1)$, $(F_{6a}^1)$, $(H_7^3)$, $(I_{17a}^2)$, $(H_9^3)$, $(I_{5a}^1)$, $(H_{10}^3)$, $(I_{18a}^2)$, $(I_{23}^2)$, $(I_{7a}^1)$, $(I_{24}^2)$, $(I_{8a}^1)$, $(I_{25}^2)$, $(I_{9a}^1)$, $(I_{39}^2)$, $(I_{10a}^1)$

- hp-graphics with a nilpotent elliptic point: $(F_{6b}^1)$, $(I_{5b}^1)$, $(I_{7b}^1)$, $(I_{8b}^1)$, $(I_{10b}^1)$, $(I_{11a}^1)$

- hh-graphics with a nilpotent elliptic point: $(I_{9b})$, $(I_{11b}^1)$

**Graphics to be done and probably easy.**

- Semi-hyperbolic graphic: $(I_{16a}^2)$

- hp-graphics with a nilpotent elliptic point: $(I_{17b}^2)$, $(I_{18b}^2)$, $(I_{26}^2)$, $(I_{40}^2)$

- hh-graphics with a nilpotent elliptic point: $(H_4^1)$, $(H_8^3)$, $(H_{12}^3)$, $(H_{15}^3)$

**Open cases.**

- Graphics with a nilpotent saddle: $(F_5^1)$, $(I_{14}^1)$

- pp-graphics with a nilpotent elliptic point: $(H_7^1)$, $(F_{7a}^1)$, $(H_{11}^3)$, $(I_{6a}^1)$

- hh-graphics with a nilpotent elliptic point: $(H_5^1)$, $(F_{7b}^1)$, $(H_{13}^1)$, $(I_{6b}^1)$, $(H_{13}^3)$, $(H_{14}^3)$

- The four additional cases: $(H_4^1)$, $(H_5^1)$, $H_{12}^3)$, $(H_{13}^3)$

- Graphics with a nilpotent point of multiplicity 4: $(I_1^1)$, $(I_2^1)$, $(I_3^1)$, $(I_4^1)$

- Degenerate graphics: $(DH_1)$, $(DF_{1a})$, $(DF_{1b})$, $(DH_2)$, $(DF_{2a})$, $(DF_{2b})$, $(DH_3)$, $(DF_{3a})$, $(DF_{3b})$, $(DH_4)$, $(DF_{4a})$, $(DF_{4b})$, $(DH_5)$.

# References

[1] L. Sylow, and S. Lie, *Œuvres complètes de Niels Henrik Abel*, Christiana, Imprimerie de Grøndlhal & Son, Johnson Reprint Corporation, 1965.

[2] R. Bamon, Quadratic vector fields in the planr have a finite number of limit cycles, *Inst. Hautes Etudes Sci. Publ. Math* **64** (1986), 111–142.

[3] L. Cairo, H. Giacomini, and J. Llibre, Liouvillian first integrals for the planar Lotka-Volterra system, preprint, (2002).

[4] C. Christopher, and C. Rousseau, Normalizable, integrable and linearizable saddle points in the Lotka-Volterra system, preprint CRM (2003).

[5] C. Christopher, P. Mardešić, and C. Rousseau, Normalizable, integrable and linearizable points in complex quadratic systems in $C^2$, preprint CRM (2002), to appear in J. Dynam. and Control Syst.

[6] F. Dumortier, M. El Morsalani, and C. Rousseau, Hilbert's 16th problem for quadratic systems and cyclicity of elementary graphics, *Nonlinearity* **9** (1996), 1209-1261.

[7] F. Dumortier, A. Guzmán, and C. Rousseau, Finite cyclicity of elementary graphics surrounding a focus or center in quadratic systems, *Qual. Theory Dynam. Syst.*, under press.

[8] F. Dumortier, Y. Ilyashenko, and C. Rousseau, Normal forms near a saddle-node and applications to the finite cyclicity of graphics, *Ergod. Theor. Dyn. Systems* **22** (2002), 783–818.

[9] F. Dumortier, R. Roussarie, and C. Rousseau, Hilbert's 16-th problem for quadratic vector fields, *J. Differential Equations* **110** (1994), 86–133.

[10] F. Dumortier, R. Roussarie, and C. Rousseau, Elementary graphics of cyclicity 1 and 2, *Nonlinearity* **7** (1994), 1001–1043.

[11] F. Dumortier, and R. Roussarie, Canard cycles and center manifolds. With an appendix by Chengzhi Li, *Mem. Amer. Math. Soc.* **121** (1996), no. 577.

[12] F. Dumortier, and R. Roussarie, Multiple canard cycles in generalized Liénard equations, *J. Differential Equations* **174** (2001), 1–29.

[13] J. Ecalle, *Les fonctions résurgentes*, Publications mathématiques d'Orsay, 1985.

[14] A. Fronville, A. Sadovski, and H. Żołądek, Solution of the 1:-2 resonant center problem in the quadratic case, *Fundamenta Mathematicae* **157** (1998) 191–207.

[15] A. A. Glutsyuk, Confluence of singular points and nonlinear Stokes phenomenon, *Trans. Moscow Math. Soc.*, **62** (2001), 49–95.

[16] A. Guzmán, and C. Rousseau, Genericity conditions for finite cyclicity of elementary graphics, *J. Differential Equations* **155** (1999), 44–72.

[17] S. Gravel and P. Thibault, Integrability and linearizability of the Lotka-Volterra system for $\lambda \in Q$, *J. Differential Equations* **184** (2002), 20–47.

[18] H. Hukuhara, T. Kimura, and T. Matuda, *Équations différentielles ordinaires du premier ordre dans le champ complexe*, Math. Soc. of Japan, 1961.

[19] Y. Ilyashenko, Divergence of series reducing an analytic differential equation to linear normal form at a singular point, *Funct. Anal. Appl.*, **13** (1979), 227–229.

[20] Y. Ilyashenko, In the theory of normal forms of analytic differential equations, divergence is the rule and convergence the exception when the Bryuno conditions are violated, *Moscow University Mathematics Bulletin*, **36** (1981) 11–18.

[21] Y. Ilyashenko, Nonlinear Stokes phenomena, in *Nonlinear Stokes phenomena*, Y. Ilyashenko editor, Advances in Soviet Mathematics, vol. 14, Amer. Math. Soc., Providence, RI, (1993), 1-55.

[22] Y.S. Ilyashenko, and A.S. Pyartli, Materialization of Poincaré resonances and divergence of normalizing series, *J. Sov. Math.* **31** (1985), 3053–3092.

[23] A. Kotova, and V. Stanzo, On few-parameter generic families of vector fields on the two-dimensional sphere, in *Concerning the Hilbert's problem*, Amer. Math. Soc. Trans. Ser. 2, **165**, AMS, Providence, RI, (1995), 155-201.

[24] P. Lavaurs, Systèmes dynamiques holomorphes: explosion de points périodiques paraboliques, Ph.D. Thesis, Université de Paris-Sud, 1989.

[25] O. Lehto, Quasi-conformal mappings in the plane, *N.Y. Springer*, 1973.

[26] J. Martinet, Remarques sur la bifurcation nœud-col dans le domaine complexe, *Astérisque* **150-151** (1987), 131–149.

[27] P. Mardešić, R. Roussarie and C. Rousseau, Modulus of analytic classification for unfoldings of generic parabolic diffeomorphisms, preprint CRM (2002).

[28] J. Martinet, and J.-P. Ramis, Problèmes de modules pour des équations différentielles non linéaires du premier ordre, *Publ. Math., Inst. Hautes Etud. Sci.* **55** (1982), 63–164.

[29] J.-F. Mattei, and R. Moussu, Holonomie et intégrales premières, *Ann. Scient. Éc. Norm. Sup.*, $4^e$ série **13** (1980), 469–523.

[30] A. Mourtada, Projection de sous-ensembles quasi-réguliers de Dulac-Hilbert. Un cas nœthérien, prépublication, Laboratoire de Topplogie, Université de Bourgogne (1997).

[31] A. Mourtada, Projection de sous-ensembles quasi-réguliers d'Hilbert II, prépublication, Laboratoire de Topplogie, Université de Bourgogne (1999).

[32] A. Mourtada, Projection de sous-ensembles quasi-réguliers d'Hilbert III, prépublication, Laboratoire de Topplogie, Université de Bourgogne (2001).

[33] A. Mourtada, Projection de sous-ensembles quasi-réguliers d'Hilbert IV: le cas général, prépublication, Laboratoire de Topplogie, Université de Bourgogne (2002).

[34] R. Pérez-Marco, and J.-C. Yoccoz, Germes de feuilletages holomorphes à holonomie prescrite, *Astérisque* **222** (1994), 345–371.

[35] C. Rousseau, G. Świrszcz, and H. Żołądek, Cyclicity of graphics with semi-hyperbolic points inside quadratic systems, *J. Dynam. Control Systems* **4** (1998), 149–189.

[36] C. Rousseau, and H. Zhu, PP-graphics with a nilpotent elliptic singularity in quadratic systems and Hilbert's 16th problem, preprint CRM (2002).

[37] M. Shishikura, Bifurcations of parabolic fixed points, in *The Mandelbrot set, theme and variations*, Tan Lei Editor, London Math. Soc. Lecture Note Ser., **274**, Cambridge Univ. Press, Cambridge, 2000, 325–363.

[38] S. M. Voronin, Analytic classification of germs of conformal maps $(C,0) \rightarrow (C,0)$ with identical linear part, *Funct. Anal. Appl.* **16** (1982).

[39] J.-C. Yoccoz, Théorème de Siegel, nombres de Bruno et polynômes quadratiques, *Astérisque* **231** (1995),1–88.

[40] H. Zhu, and C. Rousseau, Finite cyclicity of graphics through a nilpotent singularity of elliptic or saddle type, *J. Differential Equations* **178** (2002), 325-436.

[41] H. Żołądek, The cyclicity of triangles and segments in quadratic systems, *J. Differential Equations* **122** (1995), 137–159.